OAK RIDGE NATIONAL LABORATORY LIBRARIES
3 4456 0550032 0

CENTRAL RESEARCH LIBRARY

ORNL-TM-4488

Cy 71

AQUEOUS FUEL REPROCESSING QUARTERLY REPORT FOR PERIOD ENDING DECEMBER 31, 1973

W. E. Unger
J. C. Mailen
A. R. Irvine
C. D. Watson

[redacted]

LIBRARY
REFERENCE COPY

OAK RIDGE NATIONAL LABORATORY
OPERATED BY UNION CARBIDE CORPORATION • FOR THE U.S. ATOMIC ENERGY COMMISSION

Printed in the United States of America. Available from
the U.S. Atomic Energy Commission, Technical Information Center
P.O. Box 62, Oak Ridge, Tennessee 37830
Price: Printed Copy $5.45 ; Microfiche $1.45

This report was prepared as an account of work sponsored by the United States Government. Neither the United States nor the United States Atomic Energy Commission, nor any of their employees, nor any of their contractors, subcontractors or their employees, makes any warranty, express or implied, or assumes any legal liability or responsibility for the accuracy, completeness or usefulness of any information, apparatus, product or process disclosed, or represents that its use would not infringe privately owned rights.

ORNL-TM-4488
UC-79c - Fuel Recycle

Contract No. W-7405-eng-26

CHEMICAL TECHNOLOGY DIVISION

AQUEOUS FUEL REPROCESSING QUARTERLY REPORT FOR PERIOD ENDING DECEMBER 31, 1973

W. E. Unger, J. C. Mailen,
A. R. Irvine, C. D. Watson

JUNE 1974

NOTICE This document contains information of a preliminary nature and was prepared primarily for internal use at the Oak Ridge National Laboratory. It is subject to revision or correction and therefore does not represent a final report.

OAK RIDGE NATIONAL LABORATORY
Oak Ridge, Tennessee 37830
operated by
UNION CARBIDE CORPORATION
for the
U.S. ATOMIC ENERGY COMMISSION

OAK RIDGE NATIONAL LABORATORY LIBRARIES

3 4456 0550032 0

CONTENTS

		Page
Highlights		1
1.	Shipping (Task 1)	2
2.	Receiving and Storage (Task 2)	2
3.	Head-End Processing of LMFBR Fuels (Task 3)	3
4.	Volatile Fission Product Removal (Task 4)	4
5.	Dissolution (Task 5)	9
6.	Feed Preparation (Task 6)	25
7.	Solvent Extraction (Task 7)	25
8.	Plutonium Purification (Task 8)	25
9.	Waste Treatment and Storage (Task 9)	26
10.	Off-Gas Treatment (Task 10)	27
11.	Engineering Studies (Task 11)	41

AQUEOUS FUEL REPROCESSING QUARTERLY REPORT FOR PERIOD ENDING DECEMBER 31, 1973

W. E. Unger, J. C. Mailen,
A. R. Irvine, C. D. Watson

HIGHLIGHTS

Voloxidation of irradiated $(U,Pu)O_2$ fuel in a miniature rotary voloxidizer removed up to 99.5% of the tritium in the fuel. (Sect. 4)

Ruthenium was found to catalytically reduce Ce^{4+} in nitric acid; this makes the use of Ce^{4+} as a PuO_2 dissolution promotor unlikely. Fluoride still looks attractive and should cause no solubility problems with either rare earths or plutonium in any part of the processing plant. (Sect. 5.1)

A tumbling dissolver was found to be very effective in washing simulated fuel residue from chopped cladding. (Sect. 5.1)

Development of the Iodox process was continued with a series of runs made in a five-plate bubble-cap tower 7.6 cm in diameter. Stage decontamination factors averaged approximately 4 for CH_3I at an air rate of 56 liters/min. (Sect. 10.1)

Laboratory studies of the chemistry of the Iodox process increased the understanding of the equilibrium and reactions involved in the iodine—nitric acid—nitrous oxide system. It was found that methyl iodine is rapidly broken down into iodine and methyl nitrate. (Sects. 10.2 and 10.3)

The krypton removal pilot plant at ORGDP progressed into the initial shakedown operation stage. With minor changes and adjustments all equipment performed satisfactorily. (Sect. 10.4)

1. SHIPPING (TASK 1)

(A. R. Irvine, L. B. Shappert, and B. B. Klima)

The objective of Task 1 is to ensure that a safe and economic method of transporting LMFBR spent fuel will be available when needed for transport of fuel from demonstration and early commercial LMFBRs. We have established in principle that a high degree of resistance to fire and impact can be obtained in a cask made of steel and fitted with special access closures and thermal shield. The major issue at this time concerns the degree of resistance to hazards that an LMFBR fuel cask must possess.

The hazard of fuel shipment resulting from potential exposure of the shipping cask to a long-duration fire could conceivably be reduced materially if a means can be developed to remove the chemically active volatile and semi-volatile fission products from a high-temperature gas stream. A proposed scheme for improving overland spent fuel shipment safety involves shipment in an impact-resistant cask that employs a gas, probably helium, as a primary coolant. The above referred to undeveloped fission product trapping system would be in an emergency vent passage from the cask interior to the environment. The trapping system should be so installed in the shipping package as to be essentially immune to damage by impact or fire. In the event of a long-duration exposure to fire, a temperature-actuated relief device would allow the gas volume in the cask to slowly vent to the atmosphere via the fission product trap. Scouting tests and a literature survey appear to be appropriate to determine whether materials might be available which would decrease the iodine, cesium, and ruthenium content of a hot gas (800°C) by two or three orders of magnitude.

2. RECEIVING AND STORAGE (TASK 2)

This task is concerned with the means for rapid, effective, economical, and safe operation of receiving and storage facilities for LMFBR fuels.

No work was performed on this task.

3. HEAD-END PROCESSING OF LMFBR FUELS (TASK 3)

(C. D. Watson)

The objectives of this task are to develop economic head-end processing steps, in preparation for Purex recovery methods, for long- and short-decayed fuels.

In this quarter, an increased emphasis was placed on the design, fabrication, and installation of disassembly equipment and shear auxiliaries. Some field tests of a preliminary nature were performed but of insufficient depth to allow firm conclusions to be made at this time. Consequently, we are temporarily deferring any discussion of data to the next quarterly report.

The program on internal sodium was renewed and bench-scale tests were started with stainless-steel-clad UO_2 pellets containing annular sodium using moist gas at various temperatures.

4. VOLATILE FISSION PRODUCT REMOVAL (TASK 4)

(J. C. Mailen and C. D. Watson)

The objective of Task 4 is to develop a head-end processing method for removing tritium from the fuel prior to aqueous processing. Based on experimental work, it appears that this objective can be met by heating the oxide fuel to about 600°C in flowing oxygen or air (this treatment is termed voloxidation). Early removal of tritium from the fuel into a relatively small volume of gas is desirable to avoid large dilution of the tritium with water in the fuel dissolution step. In addition, the oxidation treatment has the advantage of converting any residual sodium in the fuel to the oxide prior to dissolution.

This quarter voloxidation of irradiated $(U, Pu)O_2$ fuel in the miniature rotary voloxidizer successfully removed up to 99.5% of the tritium in the fuel.

4.1 Volatilization from Oxide Fuels (Task 4.1)

(J. H. Goode, W. B. Howerton, and O. L. Kirkland)

Irradiation Data. — We reported last quarter that the relative burnups of the fuel rods in ETR irradiation capsule 43-123, estimated by gamma scanning, differed from those determined by fission gas release and recovery. Complete radiochemical and heavy element mass analyses showed the estimate from the fission gas analyses were correct. The four vertically-arranged fuel rods, which contained mechanically blended $(U_{0.75}Pu_{0.25})O_{1.975}$ varied in burnup from 2.96 to 5.01% FIMA. The burnups of the natural enrichment UO_2 insulator pellets were much less (Table 4-1).

Table 4-1. Burnup of Capsule 43-123 Fuel and Insulator Pellets

Fuel Rod No.	Location in Capsule	$(U,Pu)O_2$ Fuel Burnup, % FIMA			UO_2 Insulator Burnup-% FIMA
		^{144}Ce	^{148}Nd	All f.p. RCA*	^{144}Ce
1	Bottom	4.15	4.16	1.23	0.26
2	—	5.01	4.43	1.58	0.60
3	—	4.47	—	1.51	0.56
4	Top	2.96	—	1.00	—

*Recovery of fission products (dpm/g) relative to Rod 4.

Fission Product Migration. — Each fuel rod in Capsule 43-123 was sheared into a group of segments containing the top part of the upper UO_2 insulator pellet, the fuel rod gas plenum, and top end plug (Fig. 4-1) and two other groups containing the remainder of the UO_2 insulator and $(U,Pu)O_2$ fuel pellets. Each group was dissolved and analyzed separately. Table 4-2 compares the quantities of $^3H_2$ and ^{137}Cs recovered with the quantities calculated to be in the pellets at each burnup. The fuel pellets contained less than 5% of the calculated tritium content, as expected, while the cooler insulator pellets contained 15 to 25 times the calculated quantity. The fuel pellets generally contained slightly less ^{137}Cs than calculated, while the UO_2 pellets contained 6-8 times more than calculated. Gross gamma scans of the fuel rods showed strong activity peaks at the interfaces between the fuel and insulator pellets; it is well known that cesium migrates during irradiation and condenses at cooler locations. These data suggest much of the cesium and tritium may be located within, and probably reacted with, the UO_2.

Voloxidation. — The recent incomplete (86 to 98%) release of tritium during voloxidation of stainless steel-clad segments of irradiated $(U,Pu)O_2$ is the subject of study. The small (1.75-in. ID) rotary voloxidizer was put into the hot cell to determine whether tumbling would improve the volatility of tritium from irradiated $(U,Pu)O_2$ and dislodge the oxidized fuel from the cladding. Oxidation of $(U_{0.75}Pu_{0.25})O_2$ from HEDL experiment PNL X-6 (EBR II, 5986 MWd/t, 8.4 kW/ft) at 625°C in a static bed volatilized 90% of the tritium while oxidation at the same temperature while turning 8 rpm released 98% of the tritium. The $(U,Pu)O_2$, however, did not powder or fall from the cladding; portions of a UO_2 insulator pellet present in one segment did pulverize and release most of its tritium. The intact $(U_{0.76}Pu_{0.24})O_2$ contained 2.69×10^5 dpm/g after oxidation while the powdered $(U_{0.92}Pu_{0.08})O_2$ contained 6.20×10^4 dpm/g of oxide.

The tritium in the specimens appeared to be associated with the plutonium. In the above samples the first dissolution of the intact material contained 1.27×10^6 dpm/g of Pu and that from the powder 8.0×10^5 dpm/g Pu, i.e., close to the same quantity. A second dissolution on the plutonium-rich residue from the first leach contained 2.86×10^9 dpm/g Pu. This may help explain why voloxidation did not release all of the tritium from non-homogeneous fuels. The tritium is released upon oxidation of the UO_2 to U_4O_9, but must rely on diffusion out of the PuO_2 since no oxidation is involved.

Fig. 4-2 illustrates the effect of temperature on tritium release. Higher temperatures (~625°C) released more tritium; temperatures in this range have also been found to sinter UO_2 rather than permit oxidation to U_3O_8.[1] Optimum conditions for the oxidation of sheared LMFBR prototype $(U,Pu)O_2$ fuel pellets and UO_2 axial blanket pellets must be determined with actual vendor pellets.

References for Section 4

1. W. E. Unger et al., Aqueous Fuel Processing Quarterly Report for Period Ending June 30, 1973, Sect. 4.1, ORNL-TM-4301.

ORNL DWG. 73-10015

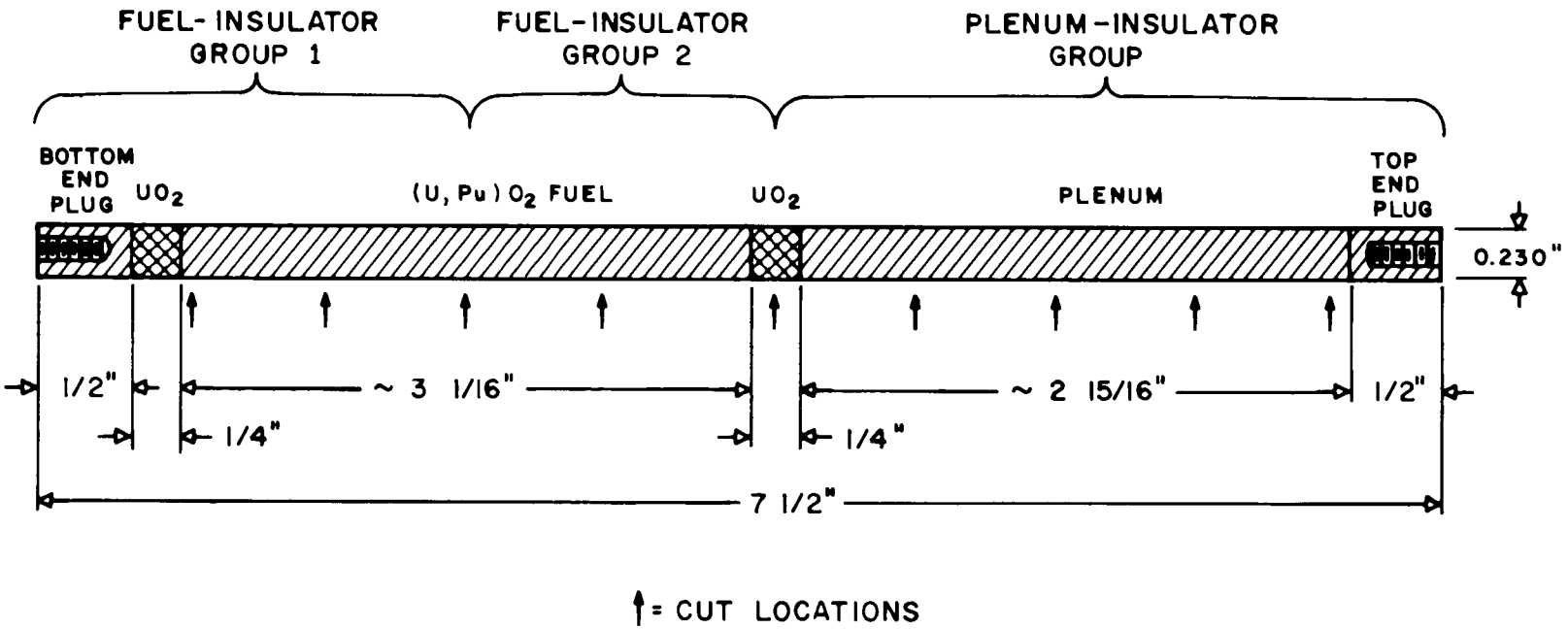

Fig. 4-1. Sectioning Diagram - Capsule 43-123 Fuel Rods.

Table 4-2. Concentration of Tritium and ^{137}Cs in UO_2 Insulator Pellets During Irradiation

Rod No.	B.U. %	Tritium-dpm/g Calculated	Tritium-dpm/g Found	^{137}Cesium-dpm/g Calculated	^{137}Cesium-dpm/g Found
1(U,Pu)O_2	4.15	2.50×10^9	4.35×10^7	3.16×10^{11}	2.74×10^{11}
1 UO_2	0.26	7.82×10^7	1.18×10^9	1.80×10^{10}	1.07×10^{11}
2(U,PU)O_2	5.01	3.05×10^9	1.52×10^8	3.85×10^{11}	3.71×10^{11}
2 UO_2	0.60	1.81×10^8	4.47×10^9	4.15×10^{10}	3.36×10^{11}
3(U,Pu)O_2	4.47	2.71×10^9	volox[a]	3.41×10^{11}	3.50×10^{11}
3 UO_2	0.56	1.69×10^8	n.d.[b]	3.89×10^{10}	2.47×10^{11}
4(U,Pu)O_2	2.96	1.79×10^9	volox[a]	2.22×10^{11}	2.11×10^{11}
4 UO_2	n.d.	n.d.	4.53×10^9	n.d.	1.85×10^{11}

[a]Fuel oxidized-tritium volatilized.

[b]Analysis not determined.

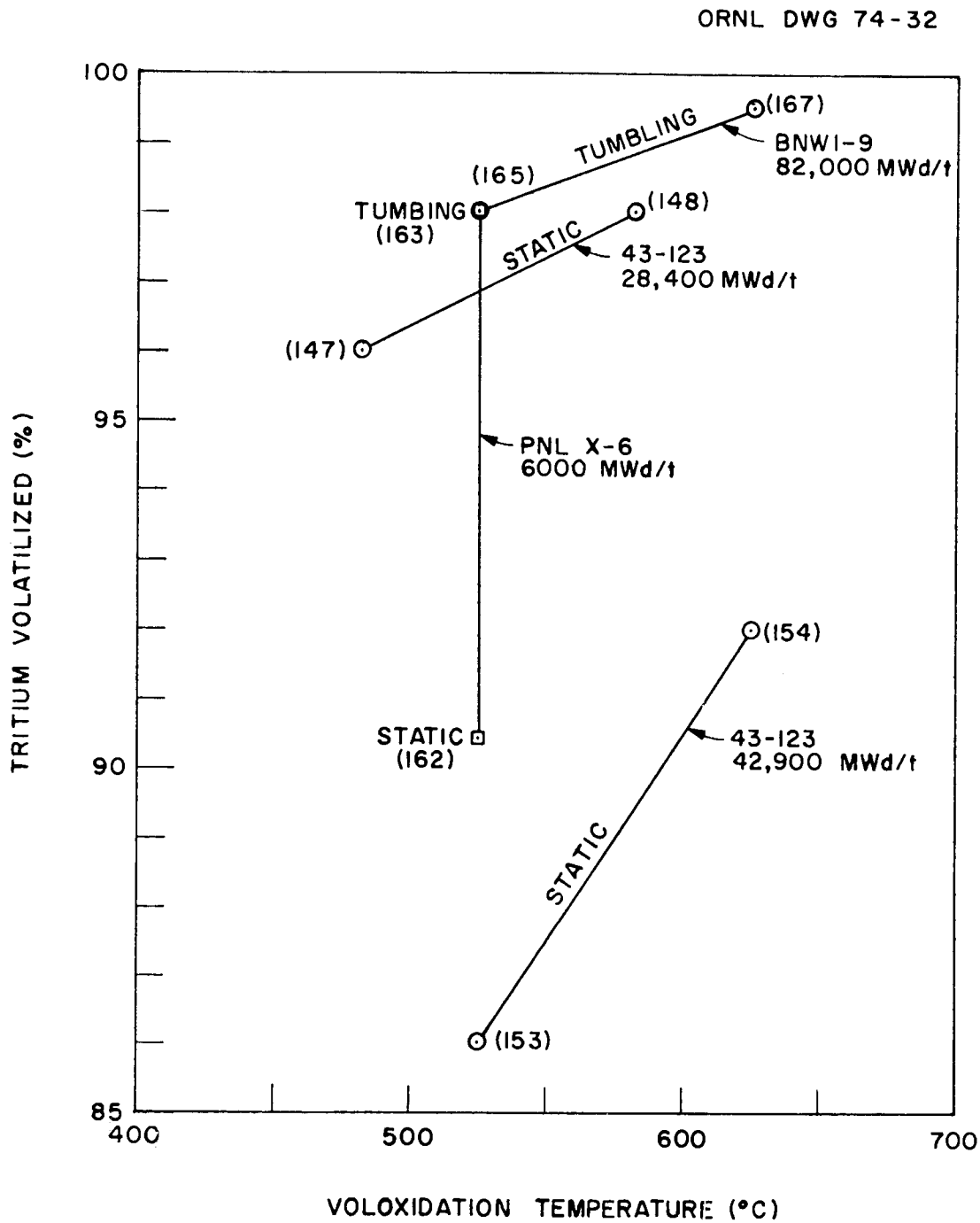

Fig. 4-2. Effect of Temperature in the Release of Tritium During Voloxidation in Air.

5. DISSOLUTION (TASK 5)

(J. C. Mailen and C.D. Watson)

The objective of Task 5 is to ensure that LMFBR fuels can be dissolved in nitric acid with high metal recoveries. Since the dissolution characteristics of the fuels can vary widely depending on their plutonium content, method of preparation, and irradiation histories, extensive leaching data are being obtained to define the effects of the many variables. A thorough understanding of iodine chemistry in the dissolver system is needed as a guide for providing effective iodine control. The dissolver equipment must be designed and operated within rather narrow limitations imposed by criticality control and off-gas considerations. It appears that satisfactory solution of these problems can best be accomplished using continuous dissolving methods and this approach is being emphasized. Evolution of a successful dissolver will require development of equipment for dependably moving the sheared stainless steel hulls and other solids through the system, and development of seals for isolating the system to prevent excessive inleakage of diluent gases.

This quarter ruthenium was found to catalytically reduce Ce^{4+} in nitric acid. Thus, Ce^{4+} cannot be used as a dissolution promotor for PuO_2 without prior removal of ruthenium. Rare earth and plutonium fluorides should not precipitate in either the secondary dissolver or in the mixed streams from the primary and secondary dissolvers if 0.1 M F^- is used to promote PuO_2 dissolution in the secondary dissolver. A tumbling dissolver was found to be very effective in washing simulated fuel residue from chopped cladding.

5.1 Dissolution of Oxide Fuels (Task 5.1)

Adverse Effect of Ruthenium on Ceric Nitrate Used as a Fuel Dissolution Promotor

(D. E.Horner and J. C. Mailen)

Use of small amounts of ceric (Ce^{4+}) nitrate, but not cerous (Ce^{3+}) nitrate, has been shown to be very effective in promoting dissolution in dilute nitric acid of PuO_2 microspheres and difficultly-soluble residues from unirradiated PuO_2-UO_2 fuel pellets. However, in many tests with residues from irradiated fuel pellets the cerium was ineffective because of essentially complete reduction of the Ce^{4+} to Ce^{3+}. Both the plutonium and uranium during dissolution reduce an equivalent amount of the Ce^{4+}; also other reductants in the system, such as nitrous acid and radiolytically-formed hydrogen peroxide, reduce Ce^{4+}. But since reduction of larger amounts of Ce^{4+} than can be accounted for by these factors alone occurred, the most likely source of reduction must have been one or more oxidizable fission products present in the irradiated residues. Mainly because of its

unique chemistry and behavior, ruthenium was investigated. Results of subsequent tests with cold ruthenium showed that this fission product could catalytically reduce greater than stoichiometric amounts of Ce^{4+} and thus was most likely responsible for the dissolution failures using irradiated fuel residues.

In a significant test, ruthenium metal (or a lower oxide) was deposited on a platinum gauze by electrolytic reduction of an acidic solution containing Ru^{3+}. Immersion of this ruthenium-coated gauze in 300 ml of a solution of 0.051 M Ce^{4+} and 4 M HNO_3 resulted in dissolution of 60 mg of the ruthenium in ∿ 0.5 hr with loss of the orange color of the Ce^{4+} and evolution of a gas (probably O_2) at room temperature and higher. The Ce^{4+} concentration had decreased to 0.0057 M, equal to a reduction of 89% of the original amount of Ce^{4+}. A portion of this solution which had set at room temperature decomposed with evolution of volatile RuO_4 which in turn apparently decomposed to form a black film of RuO_2 on the cold surface of a cover glass. Another portion of the dissolver solution was decomposed more rapidly (within 15 min.) when heated to boiling in a reflux arrangement. In this case an insoluble, black suspension of RuO_2 (identity confirmed by its ozone-like odor) formed in the solution and the remaining portion deposited on the cold surfaces of the reflux condenser. After ∿ 1 hr the Ce^{4+} concentration was < 0.0005 M, equal to > 99% loss of the original amount of Ce^{4+}. These results and their interpretation agree with the known chemistry of ruthenium, e.g., that lower valence forms of ruthenium in solution are oxidized by MnO_4^- (Ce^{4+} has a similar standard oxidation potential) and that RuO_4 decomposes readily to black, aqueous-insoluble RuO_2. The probable reactions that occurred can be represented by the equations:

(1) $Ru + 8\ Ce^{4+} + 4H_2O = 8\ Ce^{3+} + RuO_4 \uparrow + 8H^+$

(2) $RuO_4 = RuO_2 + O_2 \uparrow$

(3) $RuO_2 + 4Ce^{4+} + 2\ H_2O = 4\ Ce^{3+} + RuO_4 \uparrow + 4H^+$

With these types of reactions, a mechanism is possible whereby ruthenium can be alternately oxidized and reduced, resulting in continuous "catalytic" reduction of Ce^{4+}. That this type of catalytic mechanism is probably occurring is supported by the fact that the final Ce^{4+} concentration was much lower than the calculated concentration of 0.035 M assuming that only reaction(1) occurs with the RuO_4 being volatilized.

These results were confirmed in the subsequent tests described below. It can be concluded that the use of Ce^{4+} as a dissolution promotor for difficultly-soluble fuel residues would not be feasible unless some practical method could be found to remove all the ruthenium from the residue prior to or during the dissolution.

Hot Cell Dissolution Tests
(J. H. Goode, W. B.Howerton, and O. L. Kirkland)

Effects of Irradiation. - We reported last quarter that irradiation had improved the solubility of the $(U,Pu)O_2$ in Capsule 43-123. Figure 5-1 illustrates this effect, and points out the large variations in solubility produced by different linear heat ratings (and burnups) over the 39-in. height of the core of the ETR. (Rod 1 was the bottom rod, Rods 2 and 3 were in the peak flux region, and Rod 4, the top rod.) Figure 5-2 shows a similar effect on one fuel from HEDL experiment PNL X-4.

Effect of Ce^{4+}. - We also reported[1] that the presence of ceric ion in the nitric acid dissolvents had little effect on the solubility of PuO_2 in irradiated fuel, other than dissolving and/or volatilizing ruthenium. Ceric ion had been shown earlier to promote the dissolution of PuO_2 in unirradiated $(U,Pu)O_2$ pellets.[2]

Horner and Mailen reported in this quarterly report on the "catalytic" reduction of Ce^{4+} during dissolution of traces of ruthenium metal in nitric-acid-ceric nitrate solutions. They postulated this was responsible for the failure of the ceric ion to promote the dissolution of PuO_2 in tests with irradiated fuel specimens since large fractions of nitric acid-insoluble residues are known to be ruthenium.

We confirmed their results at room temperature, at 95°C, and at the boiling point of 4 M HNO_3--0.05 M Ce^{4+} (Fig. 5-3). The ruthenium, electroplated onto platinum gauze, dissolved with the evolution of fine gas bubbles, RuO_4 appeared in yellow droplets in the condenser, and refluxed and/or decomposed to form black RuO_2 deposits at cold spots. Ceric ion concentration was determined by reductive titration. This method of analysis gives the sum of Ce^{4+} plus Ru^{8+} oxidizing power; however, in most cases, the quantity of Ru^{8+} was relatively small. The ceric ion was reduced rapidly - particularly at the boiling point (Runs B and C) - leaving a yellow, oxidizing solution which also decreased in oxidizing power as the solution aged. (The increase in molarity on Curve A is believed due to reflux of RuO_4 into the solution.)

The RuO_2 did not dissolve in the solution; the addition of a piece of stainless steel to the 25°C yellow solution, however, resulted in deposition of RuO_2 on the stainless steel and an overnight color change from yellow (Ru^{8+}) to reddish brown (+3 or +4). In one test 2 mg of Ru reduced 15 times the stoichiometric quantity of Ce^{4+} in 2.5 hrs at room temperature.

We repeated the hot cell experiments in which electrolytic oxidation was used in an attempt to maintain cerium as Ce^{4+} during dissolution. Only ruthenium was dissolved in the HNO_3--Ce^{4+} solution in the lab tests; uranium or plutonium were not involved. The ceric

ORNL DWG 73-10012R1

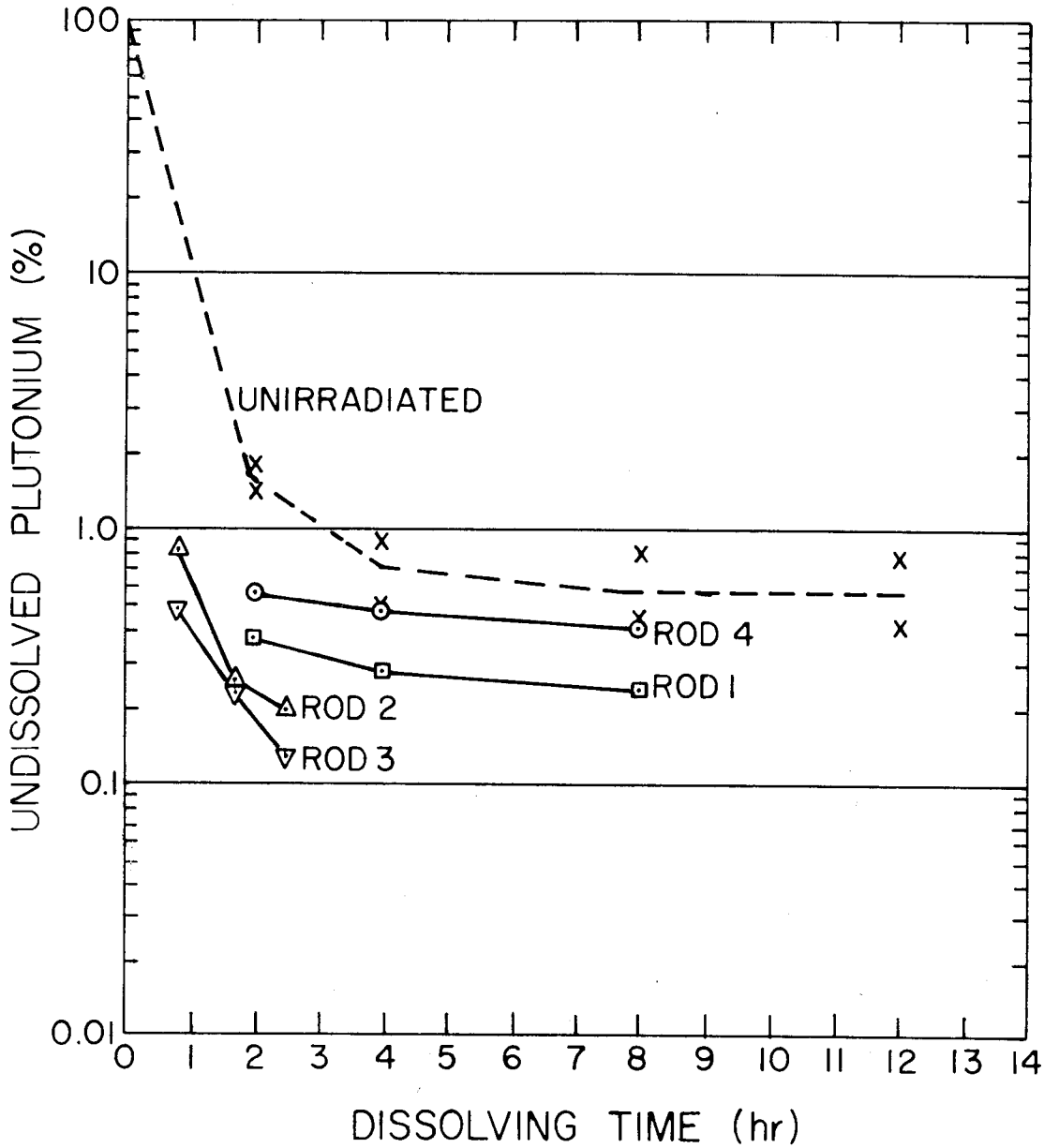

Fig. 5-1. Dissolution of Mechanically Blended 25% PuO_2–75% UO_2 in Boiling Nitric Acid (Batch FS-018 AIBIC5).

ORNL DWG 74-33

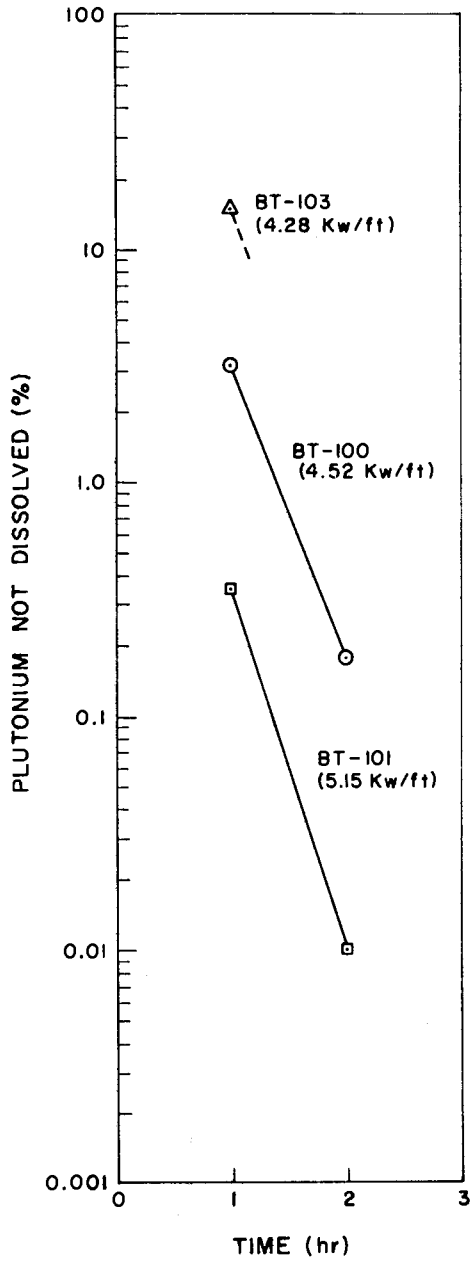

Fig. 5-2. Effect of Linear Heat Rating on Solubility of PuO_2 in PNL X-4 Fuel in Boiling 8 *M* HNO_2 (25% PuO_2–75% UO_2, Mechanically Blended, Fabrication Batch ME-21).

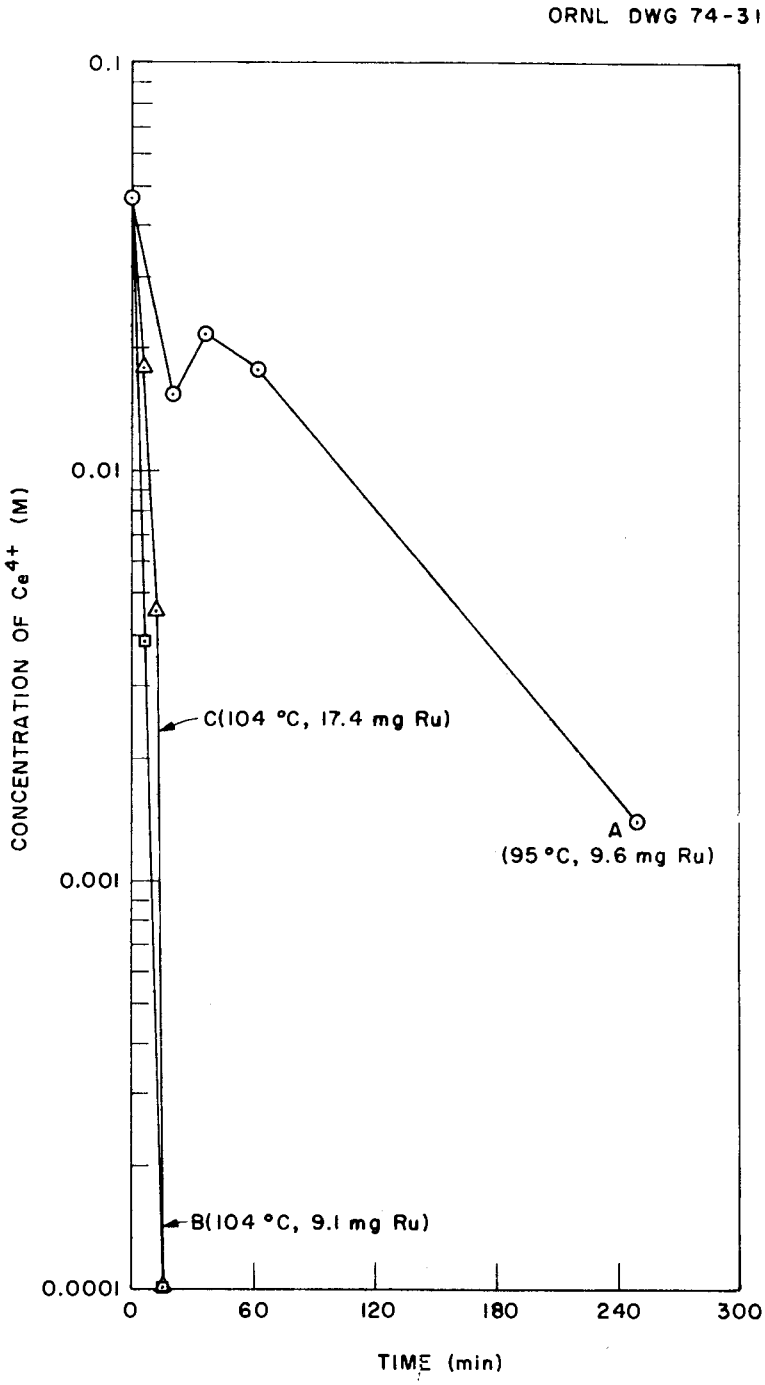

Fig. 5-3. Reduction of Ceric Ion by Ruthenium Dissolution (Temp. of Expt., Wt. Ru Dissolved).

ion was essentially (90%) gone before the solution reached boiling, just as in the hot cell test, and the 0.5 amp current did not prevent the reduction (Run C). Approximately 17 mg of ruthenium dissolved in the 14 minutes we operated. A second electrolytic test at room temperature indicated 1 amp current would reoxidize the cerium and/or ruthenium in solution, but that 0.5 amp was marginal. The oxidizing normality of the solution then decreased when the current was shut off (Fig. 5-4).

Other tests were made to determine the rate of reduction by simple boiling (essentially none), by the dissolution or corrosion of stainless steel in boiling 4 M HNO_3--0.05M Ce^{4+} (directly proportional to the dissolution of the iron), and by the presence of MoO_3, another major residue component (no effect).

Residues from the Dissolution of $(U,Pu)O_2$ in Nitric Acid. - We refluxed irradiated, mechanically blended 25% PuO_2--75% UO_2 three times in boiling 8 M HNO_3 for a total of 150 minutes. After settling, the clear supernatant from the third leach was decanted and the material washed with water. The resettled solids were washed into a wet sieve device, where the nitric-acid insoluble residue was mechanically separated by screening into five fractions; almost all of the material appeared to be $\leq$ 44 μm (-325 mesh). The complete residue contained 0.02% of the uranium and 0.05% of the plutonium from the 8.72 g of $(U,Pu)O_2$; the < 44 μm fraction, which weighed 30.3 mg, contained 0.017% of the uranium (1.0 mg) and 0.018% (0.56 mg) of the plutonium. Estimates of other elements in the -325 mesh fraction were made by emission spectroscopy: the material contained ∿ 1-4% palladium, ∿ 3-5% molybdenum, and a comparatively much larger quantity of ruthenium.

Photomicrographs showed essentially all of the < 44 μm fraction was smaller than 20 μm. Sedimentation data, based on the increase of gamma activity at the bottom of a water-filled 25-cm-long tube, indicated about 50% of the material has an apparent radius of > 8 to 10 μm. At the end of 19 hours, when the test was terminated, the apparent radius was 3.7 μm. No additional activity increase was noted, although some smaller, near-colloidal particles could have been present. These particle sizes were calculated using the density of 12.1 g/cm^3 reported by Poole, DeMent, et al., in TRG Report 1582(D). They dissolved irradiated $(U,Pu)O_2$ in 6.5 M HNO_3, and analyzed ∿5 μm diameter particles which had about the same composition as the "metallic inclusions" found with the scanning electron microscope at grain boundaries, i.e., 39 w/o Mo, 30 w/o Ru, 14 w/o Tc, and 7 w/o Rh. (This composition is nearly proportional to the fission yields for these elements.)

The particle sizes measured in our work are those from "fair" fuel, that is, from $(U,Pu)O_2$ that left about 0.5% of the plutonium insoluble in 8 M HNO_3 prior to irradiation. "Poor" fuel may leave larger chunks of plutonium-rich residue.

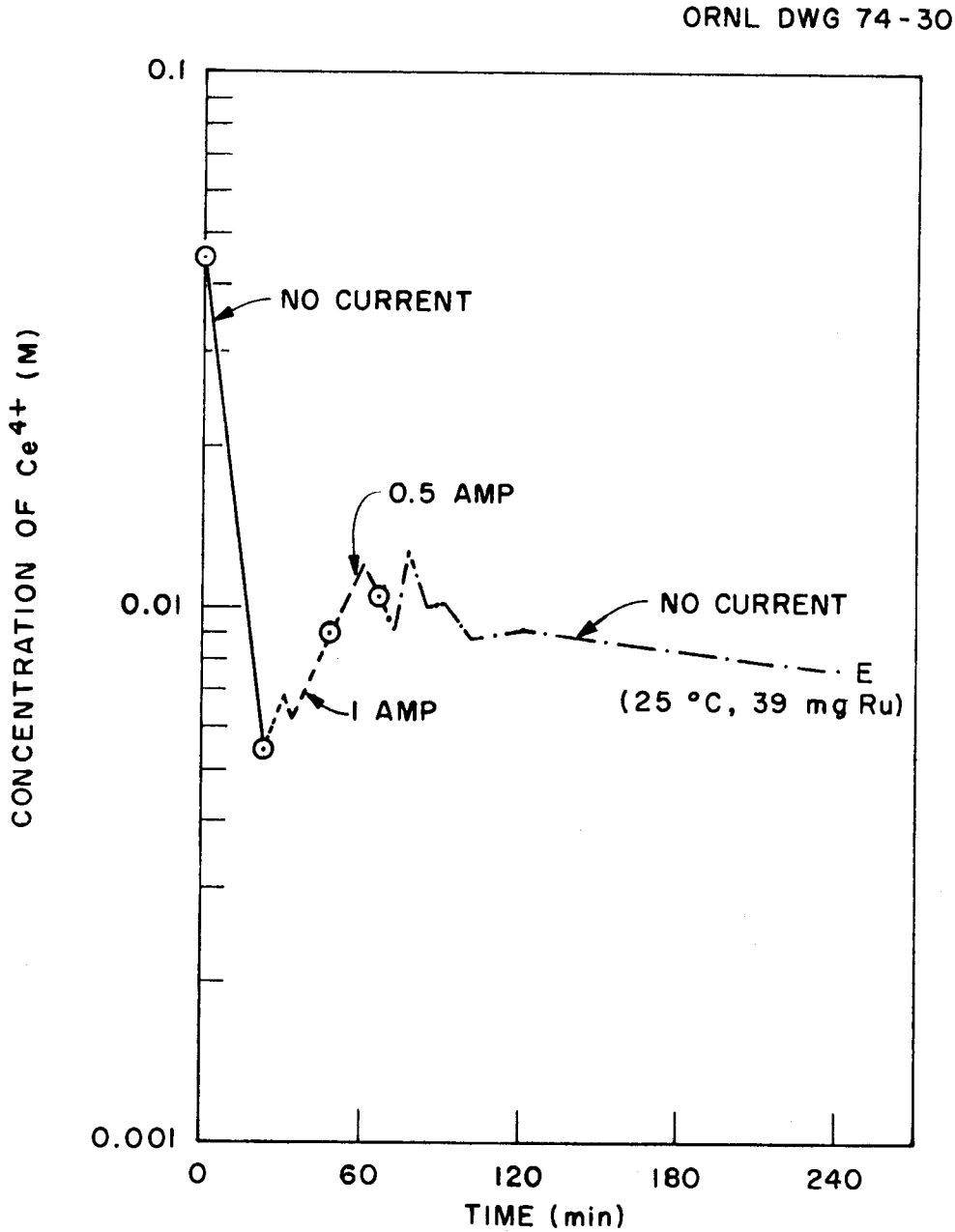

Fig. 5-4. Reduction of Ceric Ion By Ruthenium and Electrolytic Reoxidation (Temp. of Expt., Wt. Ru Dissolved).

On summary, our best estimates at this time for the characteristics of the undissolved residue from a typical "fair" fuel are:

Density	12 g/cc
Composition	Mo-Ru-Pd-Rh-Tc-Sb oxides
Amount	∿ 0.4-0.5% at 25,000-50,000 MWd/t, ∿ 1.9% at 137,000 MWd/t
Size Range	50% 8-11 μm 95% ≥ 2-5 μm

Solubility Studies of Plutonium and Rare Earth Fluorides
(D. E Horner and J. C. Mailen)

With the assumption that fluoride will be used in a secondary dissolver to promote dissolution of difficultly-soluble fuel residues, an important consideration is to determine whether the saturation solubilities of the rare earth and plutonium fluorides are high enough to preclude their precipitation in the secondary dissolver or in the combined dissolver streams.

Results of three solubility tests using cerium (3) fluoride as representative of all rare earth fluorides show that the maximum solubility in simulated dissolver solutions may be approximately three times greater than the concentrations of total rare earths expected (0.025 M) in the combined dissolver streams. In the first test, 3 moles of fluoride per mole of Ce^{3+} was added (as 1 M NaF solution) to a simulated dissolver solution containing 0.025 M Ce^{3+}--1 M $UO_2(NO_3)_2$--2 M HNO_3--0.3 M H_3BO_3 with no evidence of precipitation. In the second test, CeF_3 as a slurry prepared by precipitating it from aqueous solution, was added to a portion of the dissolver solution (∿ 22°C) and the mixture agitated overnight. Analysis of a centrifuged sample of the supernate showed the Ce^{3+} concentration was 0.065 M. This concentration, however, was most likely not the saturated concentration (longer contact times may be necessary to reach the saturation concentration). This was confirmed in the third test in which CeF_3 was precipitated from a portion of the simulated dissolver solution initially containing a higher Ce^{3+} concentration (0.33 M) than the nominal 0.025 M. Analysis of a centrifuged sample showed in this case that the Ce^{3+} concentration in solution (∿ 22°C) was 0.082 M (in this test the final concentrations of the solution components were only one-half of the original concentrations because of dilution with an equal volume of 1 M NaF solution). From these results, it can be concluded that precipitation of rare earth fluorides will not occur in the process streams, and in particular the combined dissolver streams where the final fluoride concentration may be only 0.003 M.

Rough estimates of the saturation solubility of PuF_4 in 3 M HNO_3 were made by calculating a solubility product constant based on previous experimental data and then calculating the maximum solubility concentration of Pu^{4+} corresponding to various fluoride concentrations. At a nominal fluoride concentration of 0.003 M in the combined

dissolver streams, the calculated Pu^{4+} concentration was very high ($\sim 10^5$ M), showing that there would be no precipitation problem at this point. In the secondary dissolver the calculated maximum Pu^{4+} concentration (at room temperature) that could exist with 0.1 M F^- is at least 0.3 M (or $\sim$ 72 g/liter). At lower F^- concentrations and at higher temperatures the tolerable Pu^{4+} concentration might be even higher.

Primary Dissolution Studies
(R. B. Heimdahl and D. A. McWhirter)

The investigation of flow problems associated with various primary dissolver concepts having possible application to the LMFBR aqueous fuel reprocessing program was continued. This quarter emphasis was placed on the rinsing of particulates from a static bed of hulls and the results compared with those obtained in a rotary bed. For this purpose, a static bed hull rinsing test loop was designed and installed, along with a compartmented rotary drum dissolution unit. Preliminary rinsing studies were made in both units.

The results of the rinse tests conducted with the static bed were discouraging, in that very poor rinse efficiencies were obtained. However, it was found that the rotary unit tested performed quite well in the preliminary rinse studies, and further development work will be directed toward a similar unit.

The purpose of the static bed hull rinsing loop was to simulate the rinsing or washing of insoluble particles from stainless steel hulls and wire spacers typical of the sheared product from the 250-ton shear. Other studies[2] have indicated that up to 25% of the PuO_2 in the mechanically blended UO_2-PuO_2 fuels is essentially insoluble in HNO_3. To recover this insoluble fraction of PuO_2 requires its separation and transport from the stainless steel hulls and dissolution in a more corrosive environment. The characterization of these insoluble particles was not very advanced or defined at the outset of this study, with little known but their approximate maximum size, which was considered to be -325 mesh (44 μm). Several materials were considered for use as stand-in particles with which to conduct the rinsing tests. The basic requirements considered for the particles were:

(1) Density of $\sim$ 10 g/cm^3

(2) Diameter of $\sim$ 40 μm

(3) Relatively soluble in dilute acids, and

(4) Insoluble in water.

Nickel and lead powders were selected for the initial tests due to their availability and the relative ease of working with these materials, while UO_2 and ThO_2 were reserved as possibilities for future confirmation tests once the basic rinsing data were obtained.

A schematic of the static bed hull rinse test unit is shown in Fig. 5-5. The 4-in.-diam, 3-ft-long glass column is used to simulate one basket of the proposed "carousel" dissolver concept, with the associated piping providing a flow system to simulate the possible flow conditions in the basket. The normal flow of liquid through the column is downflow, with provisions for introducing water at either the top or bottom of the column. A recirculation loop, using an air lift pump for motivation, is also provided. An air sparging connection at the bottom of the column was provided for dispersing the insoluble particles and for expanding and "bumping" the bed of hulls in later tests.

The basic rinse procedure used during these tests consisted of providing a trickle flow rate yielding 24 volume changes of the glass column over a 4-hr period (0.75 liters/min), followed by a combination of drain and fill operations. These drain and fill cycles are representative of the proposed rinsing method to be used in the "carousel" dissolver concept, with superficial water velocities of from 1 to 4 ft/min.

The glass column was loaded with 5 liters of chopped, 1-in.-long, 1/4-in.-OD stainless steel hulls and spacer wires. To obtain hulls which were typical of the product resulting from the shearing and dissolution of a fueled assembly, a suitable filler material was required to prevent severe flattening or crimping of the tubes. This filler would then be removed from the tubes, leaving a typical hull. Several materials were tested for use as a filler, including dental cement, hypo, sulfur, Wood's metal, ice, hard stick candy, and bismuth. On the basis of relative ease of filling and subsequent removal and preventing excessive crimping during shearing, the most satisfactory of these materials was bismuth. Bismuth also expands $\sim$ 3% upon solidification, thus minimizing void formations in the 30-in.-long tubes which were filled with the molten metal.

Several hull rinsing tests were conducted using -325 mesh nickel and lead powders as the simulated insoluble particles. A measured mass of powder was added to the column, which was filled with water to $\sim$ 6 in. above the level of stainless steel hulls and spacer wires. The air sparging system was then used to disperse the powder as uniformly as possible, before any rinsing had taken place. A 4-hr period of downflow through the column at a water flow rate of 0.75 liter/min was the next step, with the water level in the column maintained $\sim$ 6 in. above the hulls due to the overflow arrangement. A sequence of drain and fill cycles was then used in an attempt to rinse the particles from the bed. The method used to determine the effectiveness of the rinse cycle was to dissolve the metal particles which remained in the column and analyze the solution for its metal concentration. In practice, this was accomplished by pumping a measured volume of 6 $\underline{M}$ HNO_3 into the drained column. The air lift was then used to provide circulation of the dissolvent, and the heater was energized to heat the acid to $\sim$ 70°C. Preliminary tests had indicated that dissolution of the nickel powders occurred quite readily

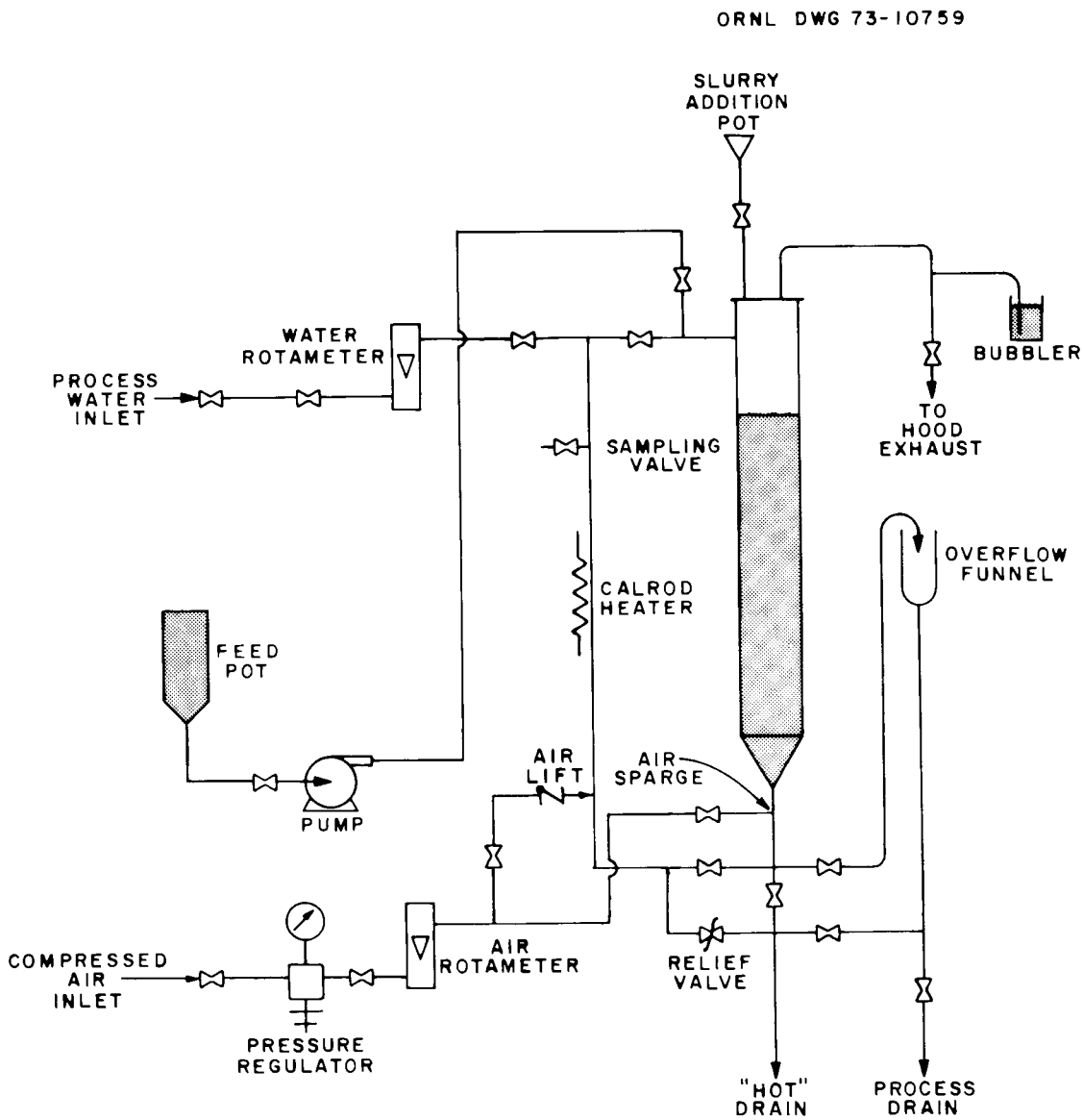

Fig. 5-5. Static Bed Hull Rinse Test Unit.

at 70°C; however, to ensure that all of the metal powder was dissolved, several samples were taken during each run to check that an equilibrium concentration was attained.

The results of the analyses for metal concentration allowed the rinse efficiency to be calculated from the relationship:

$$\text{Efficiency} = [1 - \frac{M_f}{Mi}] \times 100$$

where

M_f = mass of the metallic powder (nickel or lead) remaining in the column,

Mi = mass of powder which was added to the column.

Table 5-1 indicates the rinse efficiencies which were calculated in the tests conducted to date.

Table 5-1. Results of Rinse Tests with Static Bed

Test No.	Mi(gm)	Average Solution Conc. (mg/ml)	Rinse Efficiency (%)
SB1	10-Ni	1.49	10.6
SB2	10-Pb	1.55	7.0
SB3	10-Ni	1.47	11.8
SB4	10-Pb	1.63	2.2
SB5	5-Ni	0.70	15.9
SB6	10-Pb	1.66	0.4
SB7	25-Ni	3.40	18.2

Tests SB1 and SB3 were run at the basic flow conditions envisioned for the "carousel" type dissolver, that is, a low flow rate of water (0.75 liter/min) for 4 hr, followed by two drain and fill cycles and a final drain. In the remaining tests, various modifications or additions were made to this basic procedure. Vigorous air sparging for 30-min periods was included in all remaining tests to simulate the disturbances created by gas evolution during actual dissolver conditions. In tests SB6 and SB7, the continuous water rinse flow rate was increased by more than five times to 4.1 liters/min, and in test SB7, the column was expanded several times with short bursts of air from the sparging connection.

The results of these tests indicate that the effectiveness of removing insoluble particulates of -325 mesh from a static bed by rinsing techniques was extremely poor. In general, the use of lead

particles yielded lower efficiencies than did the use of nickel particles. This may be due to the greater density of the lead powder (11.3 g/cm^3 vs 8.9 g/cm^3 for nickel), although the lead powder also had a greater range of particle sizes. The -325 mesh nickel powder which was used was of a narrow size range of from 30 to 35 μm, while the size range of the lead particles was from 44 μm to ∿ 10 μm. Some additional rinsing tests are planned using particles of much smaller size (2 to 8 μm).

The 12-in.-diam compartmented rotary drum dissolution unit had been designed and partially constructed approximately one year ago. In the interest of exploring alternate dissolver concepts, this unit was assembled for operational tests. Basically, the unit consists of a drum having five compartments, a motor and chain-sprocket drive system, and associated piping for providing a through-flow of water.

A loading compartment, three dissolution/rinsing compartments, and an unloading compartment make up the five sections of the drum. The first dissolution/rinsing compartment and the unloading compartment have glass-pipe walls to permit visual observation of the solids-liquid interactions in these stages, as shown in Fig. 5-6. The remainder of the unit is constructed of stainless steel with the exception of the Teflon face seals on each end. The unit was designed to provide a countercurrent flow of liquid and solids, with positive control of the residence time of the solids in the dissolution/rinsing stages. The solids residence time is controlled by the design of the sloped axial transfer ducts which permit advancement of the hulls to the next compartment only while the unit is rotating in a clockwise direction. The normal, counterclockwise direction of rotation, designated as the agitation mode, is used for the dissolving/rinsing operations. After the desired residence time in a compartment, the drum is reversed in direction for one revolution, thus advancing the solids to the next compartment. Perforations in the bulkheads which separate the compartments allow the liquid to flow countercurrent to the solids.

During the initial rinse tests conducted with this unit, the rinse water was introduced at the solids discharge compartment, and allowed to overflow into a drain line at the loading compartment. The water level was kept at approximately 4 in. during these tests. Some preliminary tests were conducted to determine the rinsing capabilities of this unit. The outcome of these tests indicated that a very high rinse efficiency could indeed be obtained by using a rotary drum unit, with rinse efficiencies of > 99% easily obtainable.

The method of testing was to add a measured mass of -325 mesh nickel powder to ∿ 0.5 kg of 1/4-in.-OD, 1-in.-long stainless steel hulls and 60 mil, 1-in.-long spacer wires, in the loading compartment of the unit. A flow of rinse water was established, with the discharge being from the loading compartment. The drum was rotated in the agitation mode for a prescribed time, causing the transfer of the solids into the first stage for rinsing. After the prescribed time in the first dissolution/rinsing stage, the drum was rotated clockwise for one revolution, advancing the solids to the next stage. This cycle was repeated until the solids were discharged from the

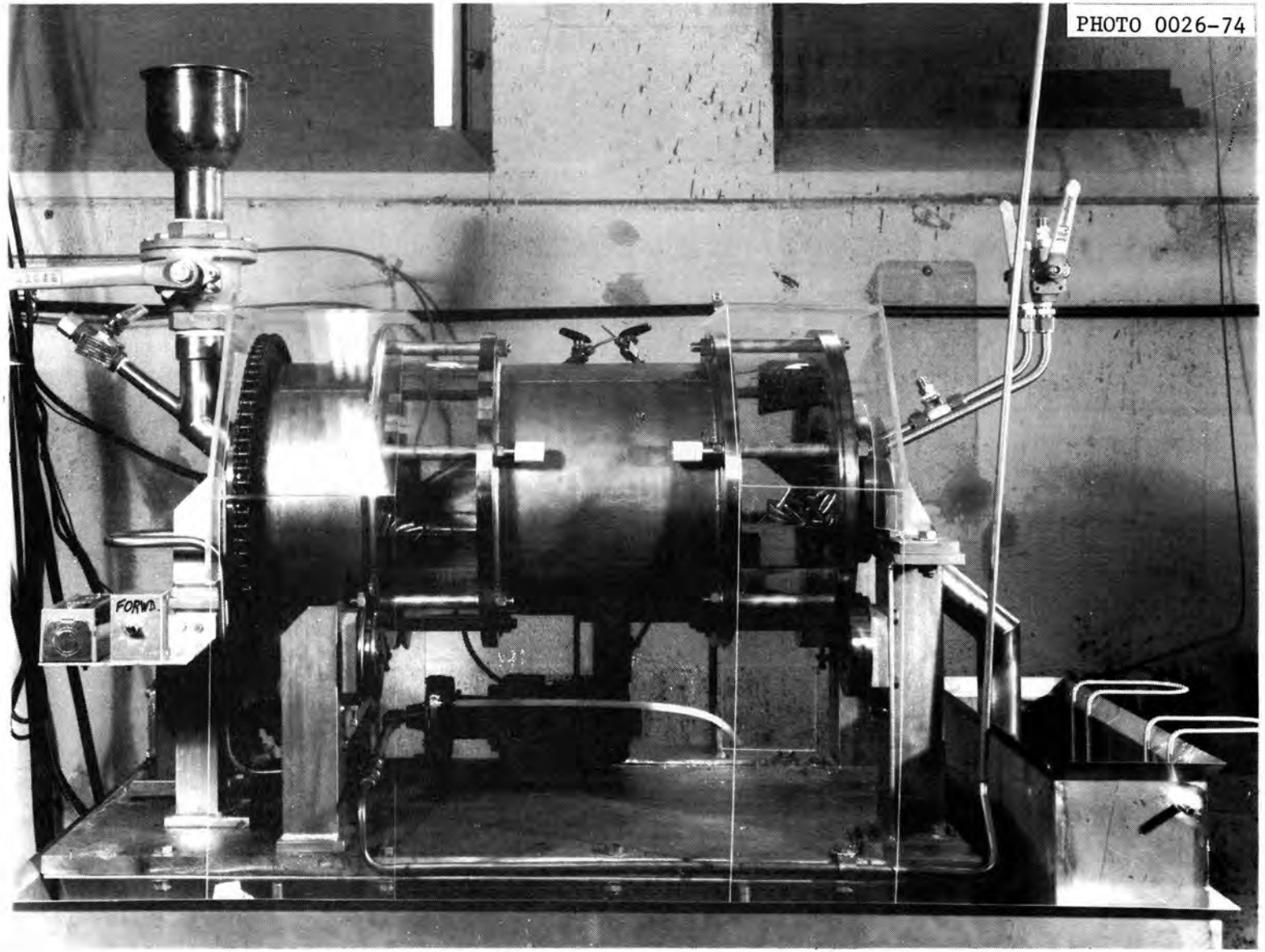

Fig. 5-6. Twelve-in.-diam Compartmented Rotary Drum Dissolution Unit.

unloading compartment and collected for analysis. The rinse efficiency was determined by leaching the discharged solids in 1 liter of 6 M HNO_3 and analyzing the solution for its nickel content. Table 5-2 indicates test conditions and results for these rinse tests.

Tests DB4 and DB5 were conducted by adding three different loads of stainless steel hulls and nickel powder in succession as the previous load was advanced to the next stage. This more nearly simulates the conditions to be encountered when operating the dissolver continuously. The effect of increasing the rinse water flow rate appears to be more important than increasing the rinsing time per stage.

Flow visualization studies were also made, using fluorescein dye and water, which demonstrated that a considerable amount of backmixing was occurring between compartments. The backmixing is caused by the pumping action of the transfer and agitation baffles in each of the stages, along with the perforations in the bulkheads, and is disruptive to the countercurrent flow of solids and liquid. Several attempts have been made to remedy this backmixing problem. These include reducing the rotational speed of the drum from 9 rpm to 5 rpm, plugging several of the perforations in the bulkheads, and increasing the free area of the transfer and agitation baffles. Each of these changes has resulted in a reduction of the degree of backmixing observed, to the extent that it now appears that the annular clearance of $\sim$ 1/64 in. between the drum walls and the outer edge of the bulkheads is the only place for any reverse flow to occur. An attempt will be made to seal this annulus.

Work has begun on the design of a full-scale, 48-in.-diam model of a rotary dissolution unit. The main objective of this unit will be to demonstrate the ability to transport large chunks of solids, such as are expected to occur from the shearing of whole fuel subassemblies.

References for Section 5

1. W. E. Unger et al., Aqueous Fuel Processing Quarterly Report for Period Ending June 30, 1973, Sect. 5.1, ORNL-TM-4301 (August 1973).

2. W. E. Unger et al., Aqueous Fuel Processing Quarterly Report for Period Ending March 31, 1973, Sect. 5.1, ORNL-TM-4240 (June 1973).

Table 5-2. Results of Rinse Tests with Tumbling Bed

Test No.	Rinse Water Flow Rate (gpm)	Rinse Time per Stage (min)	Rinse Efficiency (%)
DB1	0.77	20	99.95
DB2	0.34	20	99.9
DB3	0.34	60	99.95
DB4-1	0.34	20	99.6
-2	0.34	20	99.7
-3	0.34	20	99.9
DB5-1	0.77	20	99.8
-2	0.77	20	99.9
-3	0.77	20	99.95

Note: Test DB1 conducted with 1/8-in.-diam hulls.

6. FEED PREPARATION (TASK 6)

(J. C. Mailen)

The aqueous feed discharged from the dissolver will contain solids (undissolved fission products, corrosion products, etc.) and will probably require clarification prior to solvent extraction. Preparation of the feed for solvent extraction also will include adjustment of the plutonium valence and the nitric acid concentration, and a treatment to remove iodine.

There was no reportable progress on this task this month.

7. SOLVENT EXTRACTION (TASK 7)

(J. C. Mailen and C. D. Watson)

The objective of Task 7 is to establish that LMFBR fuels can be processed successfully by solvent extraction methods.

Work on Task 7 has been suspended for FY 1974.

8. PLUTONIUM PURIFICATION (TASK 8)

(J. C. Mailen)

This task covers the process steps in purifying plutonium, starting with the plutonium product solution from the first Purex

cycle and continuing through preparation of a product solution of adequate purity and concentration for delivery to the fuel refabrication operation.

Work on Task 8 has been suspended for FY 1974.

9. WASTE TREATMENT AND STORAGE (TASK 9)

Progress on this task is reported separately.

10. OFF-GAS TREATMENT (TASK 10)

(J. C. Mailen, C. D. Watson, O. O. Yarbro)

The removal of volatile fission products from process and effluent streams is an important part of LMFBR fuel reprocessing. Retention factors for iodine approaching 10^{10} are desired when processing 30-day-decayed fuel. Krypton and xenon retention factors in the range of 10^2 to 10^3 are desired.

This quarter development work on the Iodox process was continued on both a small engineering scale and in laboratory tests to further the understanding of the process. Modifications have been made to the ORGDP krypton removal pilot plant and shakedown runs are in progress for the new system.

10.1 Iodox Process Demonstration

(B. A. Hannaford and D. E. Spangler)

During the past quarter, four bubble-cap experiments were performed in the new 7.6-cm-diam, five-plate column in which methyl iodide traced with ^{131}I was scrubbed from an air stream with countercurrent 20 *M* HNO_3 at 25°C. Individual plate DF's fell generally in the range of 3 to 6 for the upper three plates and about 6 to 13 for the lower two plates. At air flow rates of from 14 to 28 std liters/min, the DF's generally converged on a value of 4.7 as the plate number increased from the bottom plate. At an air rate of 56 std liters/min, the DF measurements approached a constant value of 3.7.

The initial experiments in the bubble-cap column were hydraulic tests with air and water at 25°C which were intended to indicate the optimum value for liquid depth on the plate, consistent with the plate-to-plate spacing of 15 cm. Visual observation showed this value to be 4.2 cm; the corresponding submergence (liquid depth between the top of the bubble-cap slot and the overflow weir) was 3 cm. Subsequent tests in which 20 *M* nitric acid at 25°C replaced the water showed the same behavior.

The five-plate glass bubble-cap column was installed in Building 4501, and modifications were made to the air feed and off-gas systems to accommodate the tenfold increase in air flow rate over the 3 std liters/min flow rate which was used in the previously reported[1] 4-cm-diam packed column experiments. The principal qualitative change in the apparatus was the addition of a flowmeter to split off a 3.74 std liters/min flow of off-gas to the silver-zeolite bed (Fig. 10-1).

The four iodine scrubbing experiments were made with room-temperature nitric acid (nominally 20 *M*) fed once-through to the top of the column while air containing tagged CH_3I was fed to the bottom of the column at rates of 14 to 56 std liters/min. Results of these experiments are summarized in Table 10-1. The overall DF's for runs BCX-1 through BCX-3 were enhanced by the use of a condenser cooled with chilled water. Run BCX-4

ORNL DWG. 74-1955

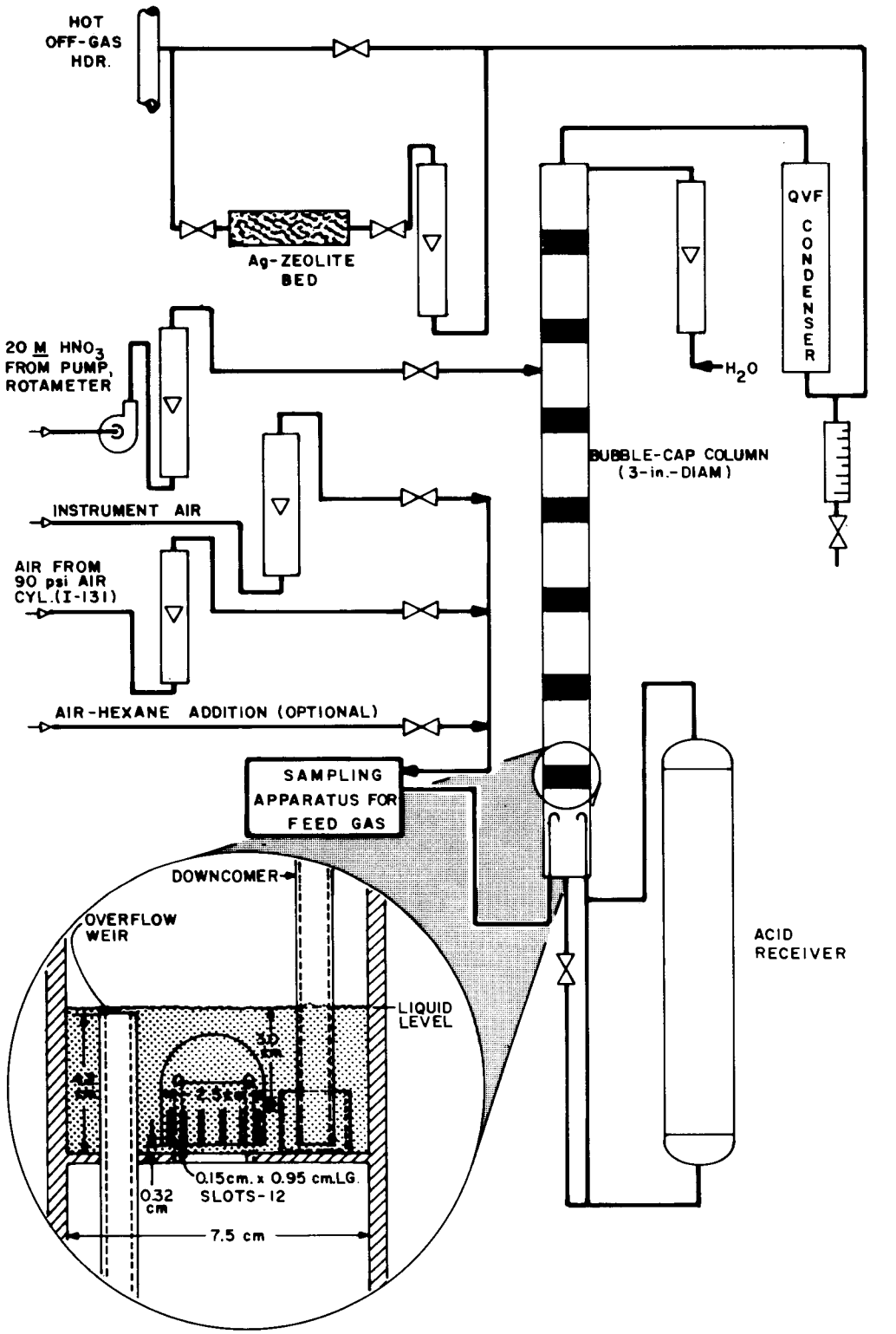

Fig. 10-1. Apparatus for Iodine Scrubbing Experiments.

Table 10-1. Summary of Methyl Iodide Scrubbing Experiments in a Five-Plate, 7.6-cm-diam Bubble-Cap Column at 25°C

Bubble-cap plate-to-plate spacing, 15 cm; slot submergence, 3 cm; and liquid holdup per plate, 0.180 liters. Steady-state run time, 40-50 min.

Run BCX-	Scrub Acid Concentration (*M*)	Scrub Acid Flow Rate (liters/min)	Air Feed Rate (liters/min)	Decontamination Factors								
				Overall	Condenser	Column	Plate 1	Plate 2	Plate 3	Plate 4	Plate 5	Average
1	19	0.020	28	2.4×10^5	100	2.4×10^3	3.3	6.2	5.1	5.0	4.7	4.74
2	20	0.039	56	1.1×10^4	35	330	4.7	3.4	2.9	2.7	2.7	3.20
3	20	0.033	14	5×10^5	25	2×10^4	12.9	8.0	7.0	5.9	4.7	7.3
4	21.6	0.041	28	2×10^4	--[a]	2×10^4	10	9.2	5.6	4.7	9.1	7.4

[a] No condenser in use; water scrubbing of acid vapor on plates 6 and 7 with water fed to plate G at a rate of 1 to 3 ml/min.

was intended to measure the effect of adding two additional plates above the acid feed plate. Water was metered to the top plate (No. 7) for the purpose of scrubbing acid vapor from the air stream. The water feed rate was lower than the rate required to reduce the acid concentration on plates 1 through 5 to 20 *M* from the feed concentration of about 21.8 *M*. Steady-state acid concentrations on plates 6 and 7 were about 16 *M* and 8 *M*, respectively.

At air rates of 14 and 28 std liters/min, the plate DF's tended toward a value of about 4.7. The relatively low DF for plate 1, run BCX-1, probably was a result of the iodine precipitation which occurred on plate 1 in this experiment.

The lower plate DF's measured for relatively high-velocity air flow, run BCX-2, suggested perhaps a loss of contacting efficiency or liquid entrainment from plate to plate. Entrainment appeared to be an unlikely explanation, based upon correlations in the literature for entrainment and superficial gas velocity. This was confirmed by entrainment measurements which were made subsequently, at air flow rates of 14, 28, and 56 std liters/min. A concentration gradient for ^{131}I was established in the column, and liquid samples (20 *M* HNO_3) were taken from each plate in the column at intervals over a 60-min period. Iodine-131 counting measurements on these samples showed that entrainment at 14 and 28 std liters/min air flow was essentially zero. At an air flow rate of 56 std liters/min, the entrainment was $\sim$ 0.8 ml/min from each plate, which was equivalent to 2% of the 39 ml/min acid feed rate for run BCX-2. The calculated effect of this entrainment on the experimentally determined decontamination factor was a decrease of about 5.3%.

A comparison of the DF data for plates 1 and 2 with data reported by Cathers for a two-plate column shows fairly good agreement. Decontamination factors for BCX-4 were 10 and 9.2 for plates 1 and 2, respectively (Table 10-1). By comparison, the average DF values for the two-plate column were 9 and 10 in two separate experiments.[1] Taken alone, this observation suggests that bubble-cap column performance is relatively insensitive to the bubble-cap design and slot submergence. These parameters were as follows:

	Five-Plate Column	Two-Plate Column
Bubble cap	Single cap, 0.15-cm slots	Triple cap plates, 0.15 cm slots
Submergence	3 cm	7.5 cm

In order to determine whether individual plate DF's have leveled out at the fifth plate, two upper plates were added so as to permit operating all seven plates with 20 *M* nitric acid in future experiments.

10.2 Reactions Between Organic Iodides and Nitric Acid - Iodox Process

(J. C. Mailen, W. E. Clark, and C. T. Thompson)

Methyl Iodide. - Methyl iodide was found to react with nitric acid to liberate iodine. The reaction is first order with respect to methyl iodide concentration. Values of the pseudo first order reaction rate constant defined by the following equation have been determined at 25°C and are tabulated:

$$\frac{d(CH_3I)}{dt} = -k_5(CH_3I)$$

HNO_3 (*M*)	k_5 (sec^{-1})
13.8	2.6×10^{-4}
15.3	5.2×10^{-3}
15.3	7.1×10^{-3}
16.6	8.6×10^{-2}
20.0	Large

These data are fitted by the following least-squares-determined equation:

$$\ln k_5 = -93.73 + 32.51 \ln C_{HNO_3} \quad .$$

Measurement of the nitrite formed during the reaction of methyl iodide with nitric acid shows that the methyl group survives intact and that the overall reaction may be one of the following:

$$CH_3I + 1/2H_2O + 1/2\ HNO_3 \rightarrow CH_3OH + 1/2\ I_2 + 1/2\ HNO_2 \ ,$$

$$CH_3I + 1\text{-}1/2\ HNO_3 \rightarrow CH_3NO_3 + 1/2\ I_2 + 1/2\ H_2O + 1/2\ HNO_2 \ .$$

In other tests methyl nitrate was tentatively identified as the major constituent of the reaction of methyl iodide with 20 *M* nitric acid. When air containing methyl iodide vapor was passed through 20 *M* HNO_3 at room temperature, most of the methyl nitrate was retained in the acid phase while the remainder was collected in a dry ice-acetone trap in the off-gas line. The concentration of methyl nitrate in the condensate was about ten times that in the 20 *M* nitric acid, demonstrating the high relative volatility of the methyl nitrate. No methyl alcohol was detected in either the acid phase or the off-gas.

In future work we plan to positively identify the constituent believed to be methyl nitrate, to determine its fate when the acid phase is heated, and to develop safe methods for its destruction in the off-gas. All literature data indicate that there will be no buildup in the acid phase

and that destruction of the relatively low concentrations expected in the off-gas will be relatively simple and quite safe.

Iodobenzene. - The literature indicates that the first step in the reaction of iodobenzene with nitric acid is the formation of a mixture of the ortho and para isomers of nitroiodobenzene. In a single test the reaction of iodobenzene with 15.3 *M* nitric acid gave a visually colorless solution with a very strong absorbance with its maximum at about 320 nm. An apparently identical absorbance peak was found for o-nitroiodobenzene dissolved in nitric acid.

10.3 Study of the Equilibrium Between I_2 and Iodic Acid in the Iodox Process

(G. I. Cathers)

The Iodox process utilizes the strong oxidizing power of concentrated nitric acid to convert elemental iodine (I_2) to the nonvolatile form of HIO_3 or its anhydro form, HI_3O_8. Studies have been made on the kinetics of this process. However, knowledge of the basic equilibrium involved could be of equal importance in recognizing the limitations of the process and how to obtain the optimum results.

If it is assumed that the major reduction product of nitric acid is nitrous acid, the following oxidation-reduction equation represents the equilibrium involved:

$$I_2 + 5HNO_3 + H_2O \rightleftarrows 2HIO_3 + 5HNO_2 \ . \qquad (1)$$

However, the presence of nitrous acid or nitrite ion is equivalent only to stating that equimolar amounts of NO and NO_2 are formed according to the following descriptive equations:

$$HNO_2 \rightleftarrows H^+ + NO_2^- \ ,$$

$$2HNO_2 \rightleftarrows H_2O + NO + NO_2 \ .$$

Equation (1) should thus be regarded as a composite equation, representing only the case where equimolar amounts of NO and NO_2 are formed, i.e., the average reduction valence of nitrogen is three. When the equilibrium is written to represent the formation of only NO, the full oxidation-reduction equation is:

$$3I_2 + 10\ HNO_3 \rightarrow 6HIO_3 + 10\ NO + 2H_2O \ . \qquad (2)$$

Another equilibrium equation could be written for the case of where NO_2 is the main reduction product.

The interaction of iodine with nitric acid is not the only one involved. The possible reduction products, NO_2, NO, or NO_2^- ion also

have some interaction with the main solvent of nitric acid. This is represented by the well-known equilibrium equation:

$$NO + 2HNO_3 \rightleftarrows 3NO_2 + H_2O \ . \qquad (3)$$

As pointed out in a previous report on the difficulty of preparation of hyper-azeotropic nitric acid, the ratio of NO_2/NO in concentrated nitric acid (above 16 *M*) at equilibrium is very high (possibly > 100/1 in 17 *M* acid). This indicates that if NO is the primary reduction product in the iodine process, the NO should be oxidized back to NO_2. However, one may still define the redox condition of the solution in terms of a reducing normality (as determined, for example, by a permanganate titration), i.e., in terms of an equivalent nitrite ion concentration.

Data on the Iodox equilibrium was obtained by means of spectrophotometric measurements using a Beckman DB-G double-beam spectrophotometer. The absorbance band at 460-480 nm was used to measure the concentration of elemental iodine, I_2. HIO_3 concentration was determined by subtracting the I_2 concentration at equilibrium from the total iodine added to the system. The interference of nitrite, or more probably dissolved NO_2 or N_2O_4, at 275-350 nm was eliminated by using nitric acid having about the same nitrite concentration as the unknown test sample in the reference cell. Equilibrium data were obtained at three nitric acid concentrations. The solutions were made up by the addition of KI solution (1 *M*), HIO_3 solution (1 *M*), and KNO_2 solution (either 5 or 12 *M*). The quantities involved were always such that equilibrium was approached from the I_2 side of the reaction. Equilibrium was usually obtained in a few hours in this case. When too much iodic acid was present in a solution, reduction back to equilibrium seemed to be much slower. The equilibrium in all solutions was of course primarily affected by the amount of nitrite present. In 14 *M* acid a small amount of nitrite was capable of holding iodine in the I_2 form. The contrary was true at 18 *M*. The procedure generally used was to measure the I_2 concentration roughly on the spectrophotometer with no nitrite in the reference. The I_2 conversion was then used to calculate the nitrite concentration, which was then placed in the reference cell for measurement of an improved I_2 conversion percentage. This was done perhaps twice in some cases; at 18 *M* HNO_3 it was found that the correct reference nitrite concentration could not be calculated (due to Eq. 1), but that it had to be formed by trial and error.

Table 10-2 summarizes all of the data obtained in terms of I_2 conversion, equivalent nitrite concentration, and the final $(IO_3^-)^2/I_2$ ratio. In order to determine the percent I_2 remaining in each solution, the molar absorbance, ϵ, had to be determined at each acid concentration. This was measured by having sufficient nitrite in solution to hold essentially all of the iodine as I_2 (added as KI, which is completely and quickly converted to I_2). The same nitrite concentration was also used in the reference cell. This was again a trial-and-error procedure. The approximate amounts of nitrite used at 14, 16, and 18 *M* HNO_3 are given in Table 10-2. Figure 10-2 is a plot of molar absorptivity versus acid concentration. The molar absorptivity decreases with increasing acid concentration and the peak shifts upwards to about 480 nm.

Table 10-2. Results of Spectrophotochemical Studies on the Equilibrium of I_2 and HIO_3 at Different Nitric Acid and Nitrous Acid Concentrations

(Solutions prepared by addition of appropriate amounts of 1 *M* KI, 1 *M* HIO_3, and/or 1-12 *M* KNO_2. Total equivalent I_2 concentration in all tests was 10^{-3} *M*. Concentration of I_2 determined by absorbance peak at 460-480 nm, with reference cell containing a NO_2^- concentration equal to that in iodine cell.)

Conversion of I_2 to IO_3^- (%)	Calc. Conc. NO_3^- ($M \times 10^4$)	Corrected HNO_3 Conc. (*M*)	Mole Ratio $(IO_3^-)^2/I_2$ ($M \times 10^4$)
14.0 *M* HNO_3			
6.39	7.4	13.97	548
15.2	8.9	13.97	189
23.5	10.6	13.97	99.6
31.3	12.5	13.97	60.3
43.2	12.7	13.97	29.9
52.4	14.0	13.97	17.3
64.0	14.4	13.97	8.1
~100	~65		
16.0 *M*			
6.23	12.5	15.97	564
9.2	16.3	15.97	358
13.2	19.7	15.97	228
19.9	22.0	15.97	129
27.5	24.0	15.97	76.5
32.2	31.1	15.97	57.1
36.3	25.5	15.97	44.7
52.6	46.7	15.97	17.1
56.0	55.0	15.97	13.8
~100	~100		
18.0 *M*			
30.6	145	17.91	63
44.5	238	17.90	27.7
52.3	184	17.88	17.4
59.0	280	17.86	11.4
65.9	327	17.85	7.06
72.7	374	17.83	4.10
~100	~800		

ORNL DWG. 74-1951

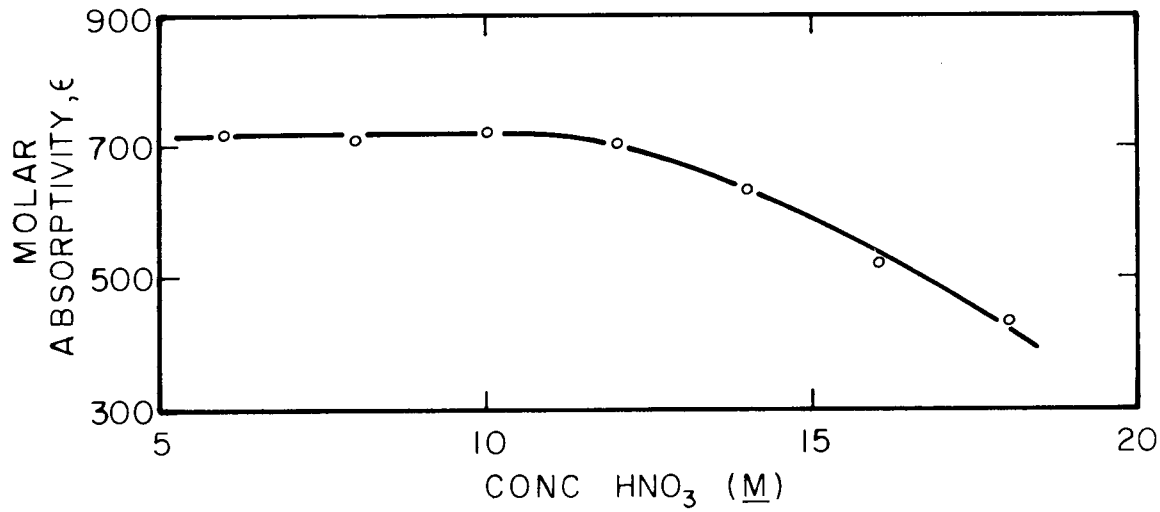

Fig. 10-2. Molar Absorptivity of I_2 in Nitric Acid.

The data of Table 10-2 is plotted in Fig. 10-3 as a test of the expression

$$\log C^2_{IO_3^-} / C_{I_2} = A - n \log C_{NO_2^-} ,$$

where n is the exponent or power of NO_2^- ion concentration controlling the iodate to iodine ratio. If derived from Eq. (1), n would be equal to 5, and this is what is found in Fig. 10-3 for 14.0 *M* acid. If derived from Eq. (2), the power dependence n would be 3.33. This compares to 2.7 and 2.5 for the slopes drawn in Fig. 10-3 for 16 and 18 *M* acid. These data suggest, therefore, that at the higher concentrations NO is formed in accordance with Eq. (2) and that this NO is then converted by reaction with HNO_3 in accordance with Eq. (3).

Another method of relating I_2 conversions in mixtures of nitric and nitrous acids involves the use of a redox potential map. Figure 10-4 shows plots of nitrite ion concentration versus the potential E, as measured at a Pt electrode against a saturated calomel electrode (SCE). Six acid concentrations were used at six different nitrite concentrations in each. Nernstian behavior seemed to be followed with a slope in accordance with the two-electron change expected for the equation

$$HNO_2 + H_2O = NO_3^- + 3H^+ + 3e^- . \qquad (4)$$

The formal potential (in water as the primary solvent) or E° for this reaction is 0.94 V as defined by the Nernst equation

$$E = E° - \frac{RT}{nF} \ln \frac{C_{NO_2^-}}{C_{NO_3^-}} . \qquad (5)$$

Extrapolation of the data in Fig. 10-4 to unit formal concentration gave the formal potentials plotted in Fig. 10-5. The plot of Fig. 10-4 therefore represents a map of the redox potential of different acid concentrations, containing some nitrite. We can relate the equilibrium data of Fig. 10-3 to Fig. 10-4 by plotting in the nitrite-ion concentrations corresponding to four fixed I_2 conversions of 25, 50, 80, and 90%. This shows in an explicit way that increasing acid strength requires a higher amount of nitrite in order to keep a fixed IO_3^-/I_2 ratio.

10.4 Selective Absorption of Krypton and Xenon

(M. J. Stephenson* and W. D. Reed*)

Preliminary shakedown and calibration of the primary ORGDP selective absorption pilot plant for removal of krypton has been completed and

---

* ORGDP.

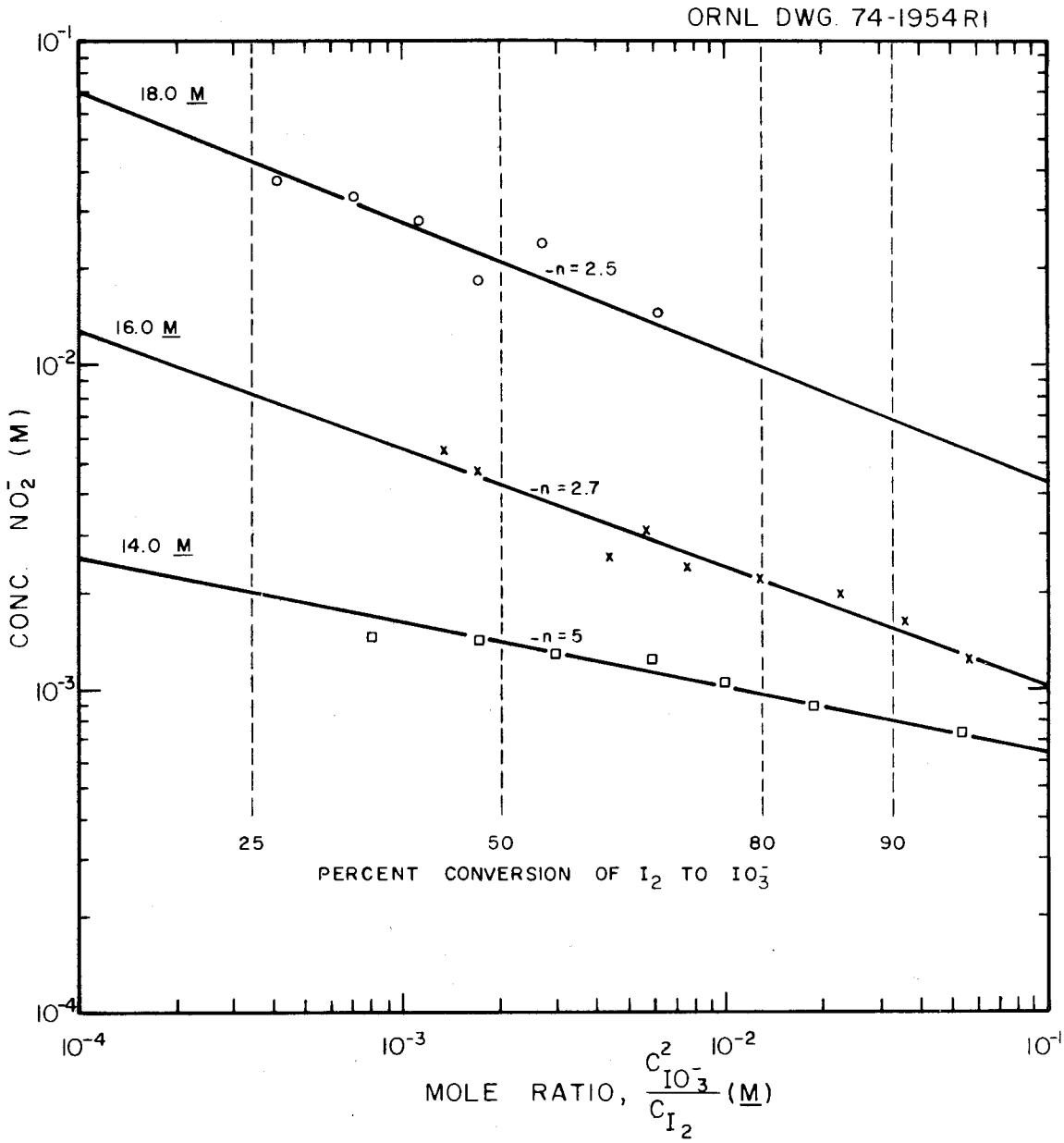

Fig. 10-3. Dependence of I_2-IO_3^- Equilibrium on Nitrous Acid Concentration.

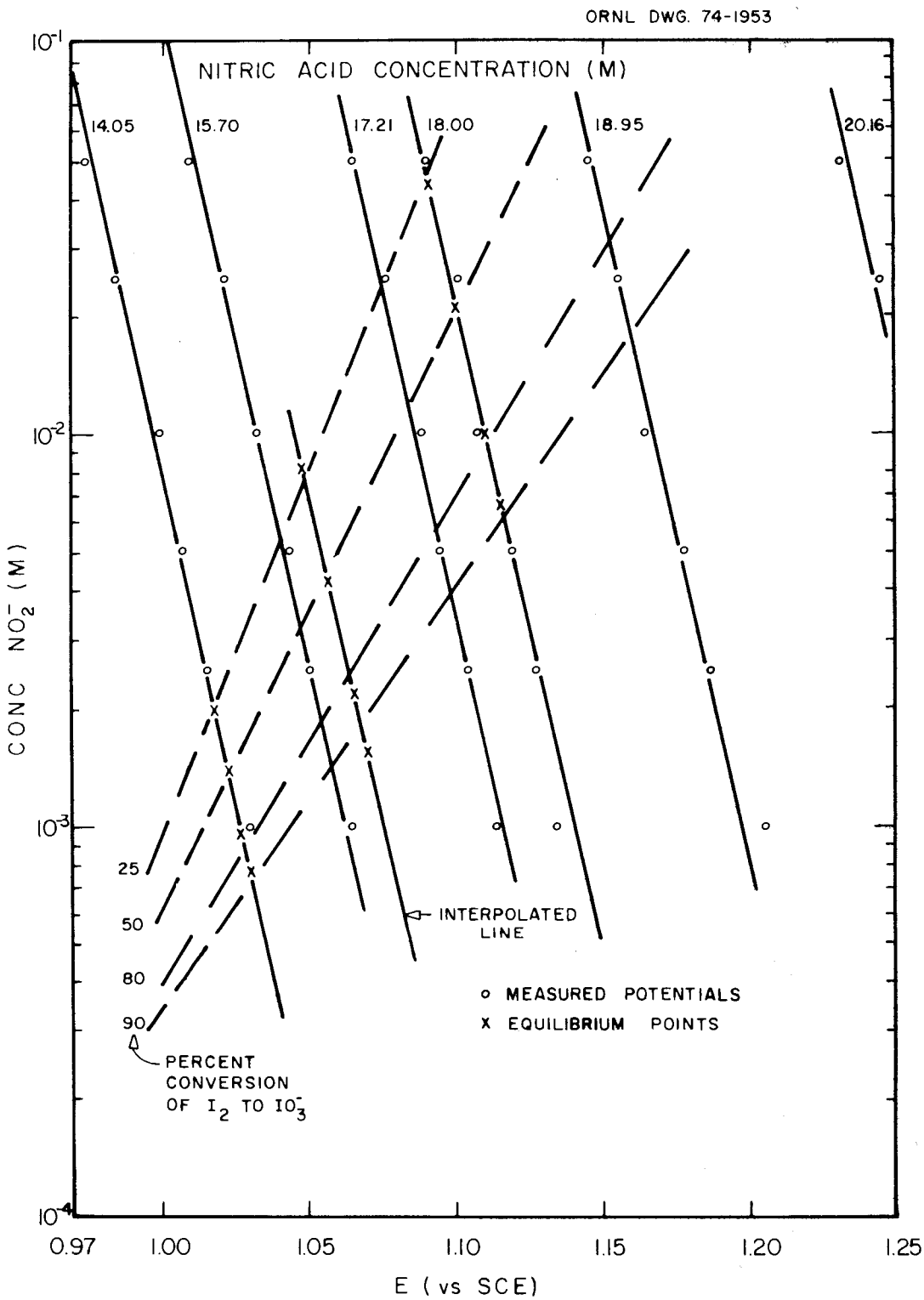

Fig. 10-4. Potential Map of HNO_3-HNO_2 System with Interpolated Potential at Different I_2 to IO_3^- Conversions.

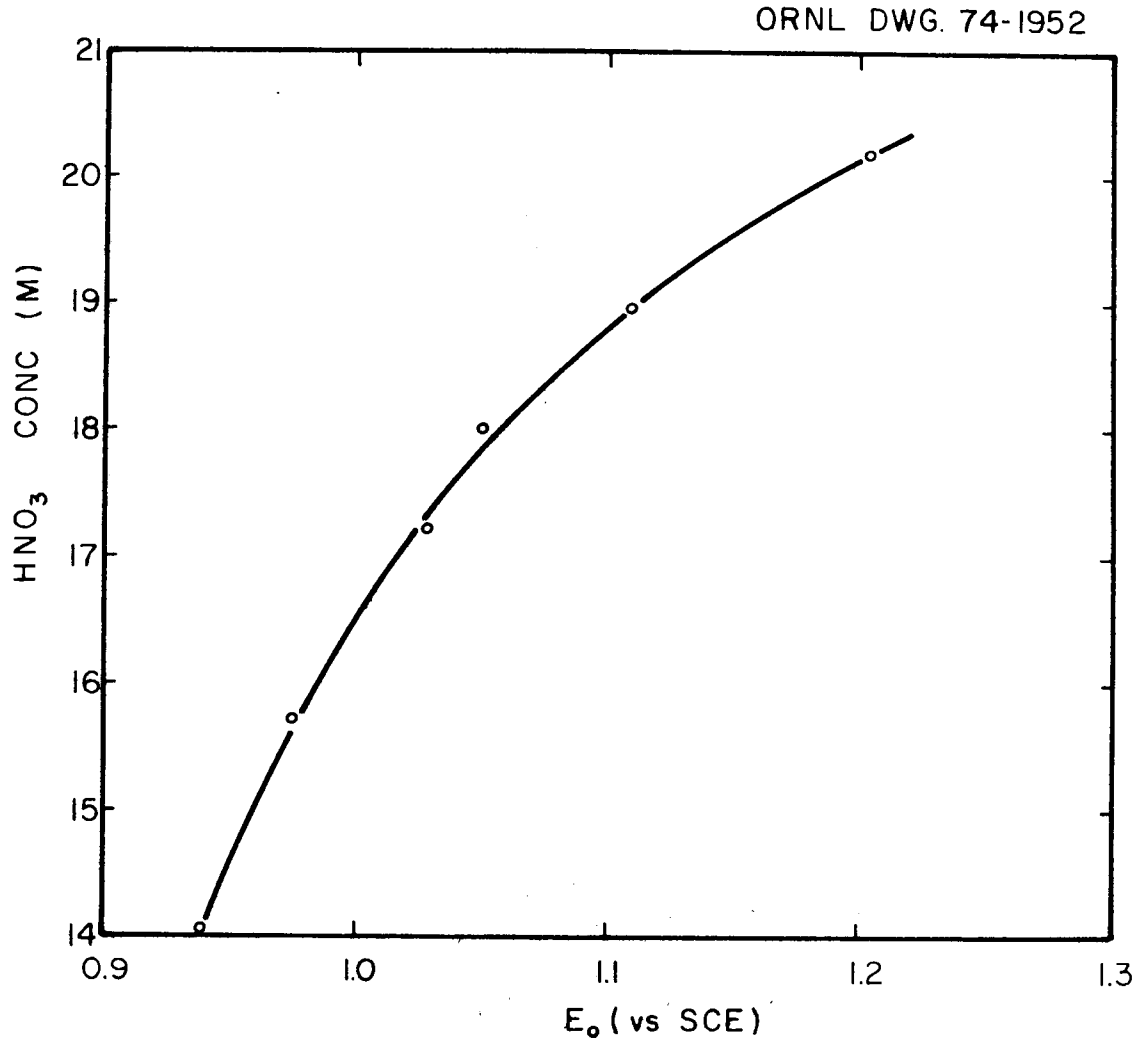

Fig. 10-5. Standard Formal Potential of the Nitric Acid–Nitrous System vs Nitric Acid Concentration.

operation of the plant is now in progress. LMFBR-related studies using refrigerant-12 as the process solvent are scheduled from January through April, while liquid carbon dioxide work for the HTGR application is planned for May and June of this year. Fabrication and installation of LMFBR auxiliary subsystems is continuing. At present, installation of the solvent purification still is being completed.

During a plant shakedown using refrigerant-12, the absorber was operated at pressures of 250 to 350 psig and temperatures ranging from minus 5 to minus 45°F. Absorber gas flows were varied from 7 to 12 scfm, while the solvent flow was maintained at 1.0 gpm. The fractionator was operated at 50 psig and stripper at 20 psig. The process diaphragm gas compressor package functioned well during the initial tests and appears to perform as claimed by the manufacturer. The two-stage, two-compressor combination delivered nearly 20 scfm during testing with an atmospheric suction and 400 psig discharge. The closed-loop, recycle flow control scheme employed to limit the compressor suction and discharge pressures can maintain tight compressor control as necessary to protect both compressors, even during the startup. The capacitance-type proportional liquid-level control systems provided good intercolumn solvent flow monitoring and control, although particular care has to be exercised during calibration. Our preliminary tests showed that each capacitance probe must be calibrated with the particular solvent to be used and at the temperature and pressure of the location. Proportional refrigeration temperature controls also provided good temperature control during shakedown with minimal system temperature fluctuation.

References for Sect. 10

W. E. Unger et al., Aqueous Fuel Reprocessing Quarterly Report for Period Ending September 30, 1973, Sect. 10, ORNL-TM-4394 (in press).

11. ENGINEERING STUDIES (TASK 11)

(A. R. Irvine and E. L. Nicholson)

The purpose of this task is to examine the overall problem of LMFBR spent fuel recovery plant design and to relate the individual problems involved in fuel recovery to the overall problem and to the other individual problems. Individual problems to be evaluated range from special problems in safety and containment (which are peculiar to reprocessing of LMFBR spent fuel) to equipment design and operational procedures.

Engineering-Scale Tests

Work was directed toward definition of the requirements for and objectives of the engineering-scale test phases of the LMFBR Fuel Reprocessing Development Program. The three engineering-scale test phases are (1) individual component or process test, (2) nonradioactive system test, and (3) a radioactive system test (hot pilot plant). The nature and purpose of the first test phase is readily apparent; its purpose is to detect and eliminate difficulties with the device or process that were not predicted on the basis of smaller-scale development work. In an unusual case, this work could bring about drastic changes in the device or even a shift to another alternative. The test work may involve operation in conjunction with adjacent pieces of equipment and will certainly require use of feeding, isolation, and discharge devices. Following is a description of the nature and purposes of the two system tests.

Nonradioactive (Cold) System Test

A nonradioactive system test would consist of protracted operation of a facility that incorporates all the reprocessing facility processes and equipment whose operation could conceivably have a bearing on the functioning of other components in the system. The major components or features to be incorporated in the facility include the following:

1. Fuel disintegration.
2. Internal sodium deactivation (voloxidation).
3. Fuel dissolution.
4. Iodine removal from dissolver product and recycle liquid streams.
5. Extraction and stripping of uranyl nitrate in an abbreviated single Purex cycle.
6. Product and waste solidification.
7. Recycle of essentially all liquids.
8. Recycle of process air and of ventilation air.

9. Leak-resistant enclosures for process equipment to simulate the confinement barriers that would exist in a radioactive facility for highly radioactive and for slightly radioactive or suspect equipment.

10. Primary iodine removal from off-gas streams. Note: This system might be abbreviated to provide only minimal contact time between nitric acid and off-gas.

11. Noble gas removal from off-gas. This system might be located remote from the main facility and operated separately using the compressed off-gas from the main facility as feed.

12. Samples of silver zeolite iodine sorbers which will be exposed to system effluent gas.

The operation of such an integrated facility will serve the following purposes:

1. A realistic approximation of the off-gas stream volume and chemical composition. Radioactive constituents will be missing. Damaging effects, if any, to sorption capacity of silver zeolite can be determined by later tests performed separately.

2. A test of isolation devices and transport mechanisms used between equipment pieces.

3. A test of treatment systems intended for removal of undesirable constituents from recycle streams. The recycle stream compositions will be more nearly representative of production plant recycle stream compositions than can be simulated otherwise.

4. Testing of special measures for improvement of plant confinement factors for liquids, gases, and solids.

5. Testing of measures to improve accountability accuracy.

6. Possible revelation of unsuspected interaction between processes.

The results of the tests, including observations of the operations will serve as the basis for design improvements which conceivably could save substantial amounts of time and money in the overall development program. This saving would accrue because the equipment modification would be made at much greater expense with equipment designed, constructed, and installed for radioactive service than with the equipment to be used in a cold system test facility.

The equipment to be installed in the cold system test facility would embody the features necessary to accomplish the process function but would not necessarily be suitable for radioactive system operation. The scale of the equipment (capacity) and major design features would be the same as anticipated for a radioactive system test facility. Although substantial

care would be exercised in equipment construction, the required quality level for use in a cold system test facility would be possibly two orders lower than required for a radioactive system test. The instrumentation used in the cold system test facility would be of the same type to be used in the radioactive system test, and much of it probably would be usable in the radioactive system.

The cold system test facility is envisioned as being comprised of two adjoining leak-resistant enclosures (simulating cell and building walls), which house the simulated high- and low-activity-level equipment, the process equipment, and an adjoining control area.

The cold system test facility will use unirradiated UO_2 in simulated fuel assemblies made of embrittled type 446 stainless steel as feed material. Thoria will likely be used to simulate nitric acid-insoluble plutonia-rich solids. Nonradioactive materials will also be added as stand-ins for the more important fission products. They will probably be added either after the simulated fuel has been chopped or to the feed to the dissolver. No plutonium will enter the facility. A possibility that is under consideration for demonstrating retention of tritium involves using deuterium as a stand-in for tritium. This is thought to possibly have greater application for demonstration of tritium confinement by water retention than by voloxidation. Both tritium retention systems could be tested simultaneously.

Radioactive System Test

The radioactive system test facility (hot pilot plant) should provide the means to test under plant conditions the new processes and equipment associated with the preparation of LMFBR spent fuel for solvent extraction, and the related processes and equipment associated with enhancement of fission product confinement. The facility should be designed such that processes and equipment intended to facilitate fission product confinement adequate for 30-day-decay reprocessing may be employed and that short-decayed fuel will be sufficiently shielded. The processing rate should preferably be relatively small such that a limited supply of fuel from a single demonstration reactor would suffice for feeding the plant at least 100 days per year. On the other hand, the equipment used in the hot pilot plant should be such as to encounter the same problems as would be encountered in a production facility. This requirement necessitates the use of essentially full-scale equipment for some operations, such as fuel disintegration and dissolution.

The equipment and process items needed for the test include all of those indicated for the cold system test facility plus certain transport and fissile monitoring systems not required or not appropriate for a cold system but required for plant operation. The high-activity-level process cell(s) should be equipped for remote maintenance. The cell ventilation system should use recirculating gas, with the capability for inert atmosphere operation. The confinement system should provide for negligible ($\leq$ 100 cfm) inleakage of air. All systems must be complete and manufactured to high standards of quality assurance; level II is probably most

appropriate for the bulk of the equipment. The solvent extraction system as well as the product and waste solidification systems should be integral with the remainder of the system in order that meaningful data can be obtained on fission product confinement and effects of fluid recycle on the various operations. All operations involving radioactive materials handling and processing should be served by a single off-gas treatment complex; these operations may include certain analytical laboratory operations.

The operation of a radioactive system test will provide vital information that cannot be obtained by nonradioactive tests or by laboratory-scale radioactive tests.

The following should be gained by a radioactive system test:

1. Confirmation of the ability to accommodate the embrittlement of fuel assembly structural materials.

2. Determination of confinement factors for iodine, tritium, noble gases, particulates, ruthenium, plutonium, and other fission products.

3. Demonstration of the ability to detect and quantify a variation in fissile content of an operating dissolver.

4. Test of the effects of fission product heating under normal and accident conditions.

5. Determination of the effectiveness of instrumentation for measuring, under plant conditions, the fissile content of leached cladding and leached noble metal fission products.

6. Test of the ability to recycle process fluids (liquids and gases) without reduction in solvent extraction system decontamination factors. This will, in effect, be a test of purification systems for recycle streams.

7. Determination of a representative plutonium loss rate.

8. Demonstration of safe dissolver operation while employing previously unused methods for nuclear safety. (Application of methods is highly beneficial for increasing capacity of dissolver system.)

9. Information pertaining to equipment reliability and process on-stream efficiency in a typical radioactive head-end reprocessing operation.

ORNL-TM-4488
UC-79c - Fuel Recycle

INTERNAL DISTRIBUTION

1. R. D. Ackley
2. R. E. Blanco
3. J. O. Blomeke
4. W. D. Bond
5. R. E. Brooksbank
6. K. B. Brown
7. F. R. Bruce
8. D. A. Canonico
9. G. I. Cathers
10. J. M. Chandler
11. S. D. Clinton
12. C. F. Coleman
13. L. T. Corbin
14. D. A. Costanzo
15. D. J. Crouse
16. F. L. Culler
17. W. Davis, Jr.
18. D. E. Ferguson
19. L. M. Ferris
20. C. L. Fitzgerald
21. J. D. Flynn
22. M. H. Fontana
23. H. W. Godbee
24. J. H. Goode
25. A. T. Gresky
26. W. S. Groenier
27. P. A. Haas
28. B. A. Hannaford
29. W. O. Harms
30. F. E. Harrington
31. R. B. Heimdahl
32. D. E. Horner
33. A. R. Irvine
34. P. R. Kasten
35. L. J. King
36. B. B. Klima
37. R. E. Leuze
38. B. Lieberman
39. A. L. Lotts
40. R. S. Lowrie
41. R. E. MacPherson, Jr.
42. J. C. Mailen
43. A. P. Malinauskas
44. W. T. McDuffee
45. L. E. McNeese
46. J. P. Nichols
47. E. L. Nicholson
48. J. R. Parrott
49. A. M. Perry
50. H. Postma
51. R. H. Rainey
52. A. D. Ryon
53. W. F. Schaffer, Jr.
54. C. D. Scott
55. L. B. Shappert
56. W. E. Shockley
57. J. W. Snider
58. M. J. Stephenson
59. D. B. Trauger
60-62. W. E. Unger
63. V. C. A. Vaughen
64. C. D. Watson
65. G. A. West
66. R. G. Wymer
67. O. O. Yarbro
68. H. C. Young
69. Laboratory Records, RC
70-71. Central Research Library
72. Document Reference Section
73-82. Laboratory Records
83. ORNL Patent Office
84. Nuclear Safety Information Center

EXTERNAL DISTRIBUTION

85. Research and Technical Support Division, AEC-ORO
86. RRD Senior Site Representative, D. F. Cope, at ORNL
87-88. Director, Division of Reactor Research and Development, U. S. Atomic Energy Commission, Washington, D. C. 20545

89-317. Given distribution as shown in TID-4500 under UC-79c, Fuel Recycle Category